catalysts

MDPI

Review

Au/CeO_2 Catalysts: Structure and CO Oxidation Activity

Miguel Angel Centeno [1,*], Tomás Ramírez Reina [2], Svetlana Ivanova [1], Oscar Hernando Laguna [1] and José Antonio Odriozola [1]

[1] Departamento de Química Inorgánica, Universidad de Sevilla e Instituto de Ciencias de Materiales de Sevilla Centro mixto US-CSIC Avda. Américo Vespucio 49, Seville 41092, Spain; svetlana@icmse.csic.es (S.I.); ohlaguna@gmail.com (O.H.L.); odrio@us.es (J.A.O.)

[2] Department of Chemical and Process Engineering, University of Surrey Guildford, Guildford GU2 7XH, UK; t.ramirezreina@surrey.ac.uk

* Correspondence: centeno@icmse.csic.es; Tel.: +34-95-4489543

Academic Editors: Leonarda F. Liotta and Salvatore Scirè
Received: 6 September 2016; Accepted: 11 October 2016; Published: 18 October 2016

Abstract: In this comprehensive review, the main aspects of using Au/CeO_2 catalysts in oxidation reactions are considered. The influence of the preparation methods and synthetic parameters, as well as the characteristics of the ceria support (presence of doping cations, oxygen vacancies concentration, surface area, redox properties, etc.) in the dispersion and chemical state of gold are revised. The proposed review provides a detailed analysis of the literature data concerning the state of the art and the applications of gold–ceria systems in oxidation reactions.

Keywords: gold–ceria catalysts; oxidation reactions; preferential oxidation reactions (PROX); water gas shift (WGS)

1. Introduction

Carbon monoxide (CO) is one of the extended pollutants of our environment, thus requiring prevention and control to insure the adequate protection of public health [1]. Carbon monoxide is hardly detectable, colorless, tasteless, odorless, non-irritating very toxic gas for humans and animals because of its high affinity to hemoglobin and the cell's oxygen transport blocking. Exposure to CO must never exceed 25 ppm in 8 h or 50 ppm in 4 h because, above these limits, important detrimental effects are observed up to the lethal concentrations of around 650–700 ppm [2]. Moreover, carbon monoxide is also a precursor of ground-level ozone, which can generate serious respiratory problems. All of these environmental issues render CO oxidation reaction the preferred option for CO depletion in polluted atmospheres.

In 1987, almost 30 years ago, the discovery of Haruta and co-workers revolutionized the concept of CO oxidation for environmental proposes [3]. They demonstrated that very small gold nanoparticles are extremely active for carbon monoxide oxidation at sub-ambient temperatures. This achievement provoked a great scientific interest converting gold in the most popular metal for the catalytic oxidation of CO [4–28]. Figure 1 shows the growing trend in a number of publications per year involving CO oxidation using gold-based catalysts. A several fold increment in the last decade of the publications with search strings "CO oxidation" and "gold-based catalysts" was observed indicating the importance of this catalytic process in heterogeneous catalysis.

A number of other possible applications for gold-based catalysts able to perform CO oxidation at room temperature appear such as carbon dioxide lasers, gas sensors, respirators for protecting firefighters, and miners from CO poisoning, air-cleaning devices, etc. [29].

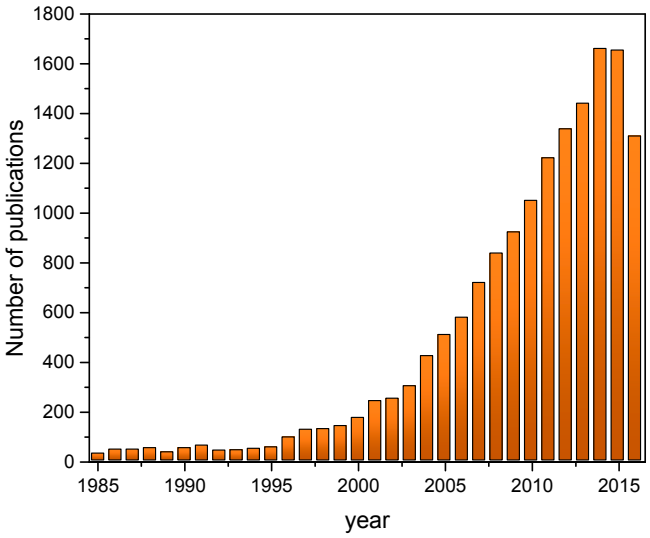

Figure 1. Number of published papers from 1985 in the Scopus Scholar database using "gold catalysts" and "CO oxidation" as search strings (September 2016).

Out of the environment protection issue, the CO abatement is also a key reaction in many industrial processes. The water gas shift reaction ($CO + H_2O \leftrightarrow CO_2 + H_2$) is one of these reactions. Despite the fact that the reaction was described at the end of the 18th century, its main applicability was not found before the 1920s, when the Haber–Bosh process for ammonia synthesis called for pure hydrogen production. From this moment on, the water gas shift (WGS) reaction gained importance and became an inseparable part of various industrial processes, such as ammonia and methanol production, hydrogen supplies for the petrochemical industry, Fisher–Tropsch reactions, and numerous reforming reactions.

Presently, a renewed interest in the WGS reaction emerges associated to the hydrogen fuel cell (FC) technologies. Hydrogen as an energy carrier is usually produced from hydrogen-containing molecules, such as hydrocarbons, ammonia, or chemical hydrides [30]. The best short-term option seems to be the hydrogen production via hydrocarbons reforming. However, the resulting products are a mixture mainly constituted by hydrogen and carbon oxides [31]. The presence of CO in the hydrogen flows, even in small amounts at the ppm level, inactivates the fuel cell electrodes. Therefore, to avoid fuel cell anode poisoning, several fuel processing steps, including CO removal by means of a WGS and CO preferential oxidation reactions (PROX) or methanation must be applied. The development of efficient catalysts for these processes is fundamental to guarantee the success of the so-called "hydrogen economy".

Among all the reported catalysts, gold-based materials have been broadly employed for the WGS reaction showing promising results in many cases [32–34]. Some of the main benefits of using gold-based catalysts include good activity in the low-temperature range, the absence of pre-treatment, and pyrophoricity. Nevertheless, these systems also show drawbacks including extreme sensibility to the preparation procedure (existence or not of gold nanoparticles), the importance of a support nature (especially development of an active gold–support interface), and relatively low catalyst stability attributed to support deactivation. However, when these parameters are carefully controlled and the support is prudently selected, gold-based materials are outstanding for the WGS reaction.

The production of hydrogen pure enough to feed polymer electrolyte membrane fuel cell (PEMFC) requires further clean-up processes after the WGS unit in order to reduce the CO concentration to compatible levels, typically 10–50 ppm depending on the cell anode [10]. The preferential CO oxidation in rich-H_2 streams (Scheme 1) has been proposed as cheap and efficient alternative for the elimination of the final traces of CO [35–38]. The oxidation is rapid and responds quickly to changes in operating

conditions, but it is essential to choose catalysts and operating conditions that minimize the oxidation of hydrogen. In this regard, control of temperature is found to be particularly important [10].

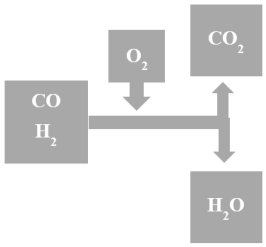

Scheme 1. Block diagram showing the possible paths for oxidizing CO–H_2 mixture.

Attending the above-mentioned scheme, the PROX reaction requires selective catalysts able to abate CO without oxidizing H_2, an undesirable side reaction. In other words, high CO oxidation activities coupled with low hydrogen ones are essential requirements for the PROX catalysts [38,39]. Various studies have confirmed that the rate of CO oxidation over supported Au catalysts exceeds that of H_2 oxidation [40–43]. Moreover, gold-based catalysts show extraordinarily high activity in the low temperature range, which is appropriate for fuel cell applications. The gold-based catalysts often result after combining this noble metal with support with the intrinsic ability for the CO abatement. Therefore, the final result is the combination of both the ability of the gold nanoparticles and that of the support for the CO oxidation. However, cooperative effects have also been observed between both components of the catalyst, promoting a catalytic performance that is something more that the mere sum of their separate abilities to oxidize CO.

Within the studied supports, usually metal oxides, there are reports about the use of MnO_x [44], Fe_2O_3 [45], and Co_2O_3 [46], among others. Their intrinsic ability for the CO oxidation is due to some oxygen species that are especially activated through electronic transfer between them and the metallic cations, allowing a successful activation of the CO and O_2 molecules for CO_2 production. For that reason, when these materials are employed as catalytic supports, they are known as active supports. CeO_2 is one of the most studied active supports due to its redox behavior achieved by the easy and reversible transformation of Ce^{4+} cations into Ce^{3+} cations. This redox property strongly depends on the mechanism followed by this solid for the oxygen vacancy formation. Oxygen vacancies are punctual defects specially established at the surface of the material [47,48] and are responsible for the ability of the CeO_2 to exchange oxygen species with the environment. In this sense, CeO_2 can be considered as an oxygen buffer due to its oxygen storage capacity [49]. It has been widely reported that the doping of the CeO_2 structure by the addition of one or more cations with a different nature, allows achieving mixed systems with improved oxygen exchange ability. Many different cations have been successfully used: Zr [11,50], Zn [17,51], Fe [52,53], Co [54], La [55,56], Eu [57], Gd [56], and Sm [58], among others. Taking into consideration the wide range of possible combinations between ceria and different cations, the different synthesis procedures that can be applied to obtain the mixed oxides, and the strict control of the variables required during the synthesis procedures, studies in the near future will be devoted to understanding the structural properties achieved for the obtained solids and to correlating them with their catalytic activity in the CO oxidation reactions, despite the large number of yet published papers in this topic many works. The transition metals are interesting and potential modifying agents of the CeO_2 lattice because they have d electrons that can interact with the unoccupied energy levels of the cerium cations [59], promoting the ionic mobility into the mixed structure.

Thus, considering the intrinsic properties of cerium oxide and that the deposition of small amounts of gold in the surface of this material allows for the obtainment of much more active systems in the CO oxidation reactions [20,23,25,60], including total oxidation, WGS, and PROX, this review

presents Au/CeO_2 catalysts as a case study and develops relevant aspects regarding the preparation, characterization, and catalytic activity evaluation of these materials, reported in the literature.

2. Preparation of Au/CeO_2 Catalysts

The last 20 years saw the pursuit of method perfection for preparing gold-based systems. Gold nanoparticles production, supported or not on ceria, is very sensitive to the preparation parameters, such as pH, concentration, use of bases, temperature, or even the presence of light. Most information regarding the advances on gold nanoparticle production and the subsequent supporting process is summarized in book chapters [40,61] and various reviews [5,8,29,32,60,62–93]. A well-established paradigm in the gold catalysis field is that the smaller the gold particles size, the higher their activity in numerous oxidation reactions. The deposition–precipitation method using either urea or bases such as sodium or potassium hydroxide or carbonate is the most preferred method to support gold nanoparticles on mineral supports [70,94–96]. The use of direct anionic exchange including an ammonia-washing step is also well represented [97–99]. Recent reports devote a substantial part of the fairly old colloidal route [100] with all its variations mainly concerning the reduction agents. This latter route starts to become important with the development of carbon-supported gold nanoparticles for selective oxidations in liquid phase [101–103]. The modification of the colloidal methods arises from the choice of the reduction agent or for the moment of its application. Besides these mostly employed conventional methods of preparation of Au/CeO_2 catalysts, new reports presenting alternative routes deserve interest. We review some of them without the sake of exhaustiveness. The approach proposed by Lakshmanan et al. [104] is one of these examples. In their proposal, glycerol acts as a reducing agent of the already preformed Au/CeO_2 precipitate. The particularity of this work is that they used glycerol not only as a gold reducer but also as a participant in the catalytic reaction. The catalyst precursor to glycerol weight ratio affects the average gold particle size and the product distribution in the selective oxidation of glycerol to lactic acid.

Another interesting approach is the use of supercritical CO_2 as an anti-solvent for the preparation of Au/CeO_2 catalyst [105,106]. The catalyst precipitates on adding the precursor solution to supercritical CO_2. This Au/CeO_2 catalyst demonstrates an enhanced activity in comparison to conventionally prepared systems, this behavior being assigned to the variation of the nucleation velocity during the catalyst preparation. Very recently, a novel method based on the photo-thermal effect generated from localized surface gold plasmon resonance (LSPR) has been proposed for preparing Au/CeO_2 core–shell structures [107]. The method benefits from the heat generated by LSPR on Au nanoparticles, which induces the polymerization reaction of the ceria precursor sol and results in ceria formation just on the Au nanoparticles surface. Mitsudome et al. [108] obtain similar Au/CeO_2 core shell structures by mixing reverse micelle solutions of Au(III), Ce(III), and NaOH. In this mixture, a redox reaction between Au(0) and Ce(IV) occurs yielding the Au/CeO_2 core shell structure. The interfacial cooperative effect of the structure results in maximal selectivity to alkenes in the reaction of selective semi-hydrogenation of various alkynes.

Bera and Hedge [109] proposed the solution combustion method to prepare Au/CeO_2 catalysts. In this method, Au remains in ionic form until a thermal treatment at 800 °C is applied. Yang et al. [110] proposed the vapor phase synthesis of Au/CeO_2 catalyst. The method consisted of vaporizing the metal target by using a second harmonic generation neodymium-doped yttrium aluminium garnet (Nd–YAG) laser on the cold top plate where the oxide support is placed. This preparation method appears to be very versatile, i.e., a variety of efficient catalysts can be designed by using simple and flexible control of different synthetic parameters.

The decomposition of a single-source precursor was also reported as a versatile method for gold catalysts preparation [111]. The method normally uses the double complex salts (DCS) of transition metals, ionic compounds for which cation and anion are coordination compounds, and appears well suited for the synthesis of bimetallic catalysts. The bimetallic catalysts may be formed either by sequential impregnation of the monometallic salts onto the support or by the impregnation of

an organic solution of a DCS. This method allows for the control of the bimetallic phase formed and hence of the catalyst activity. Another proposed method to control Au particle sizes consists in the deposition of thiol protected $Au_n(SR)_m$ nanoclusters, where n and m are the number of Au atoms and SR the thiolate ligands, respectively, where R is an alkyl group [112]. The main difference of this method with the traditional deposition precipitation one resides in the precise size of the gold thiolate clusters resulting in monomodal particle size distribution in the final material. In general, particle sizes below 2 nm, or having less than 200 atoms can be conceived. Although the activity of these systems was not satisfactory, their possible use as model catalyst for mechanistic studies could be easily envisaged.

Besides the above-mentioned preparation methods, a common strategy, very popular in the last decade, is to disperse Au/CeO_2 catalysts on high surface area supports. Generally, this strategy leads to very performant materials either with enhanced Au dispersion on the support surface or a higher surface-to-bulk ratio and therefore complete Au/CeO_2 interface exposure to the reactants. The latter effect is observed when the size of both gold and CeO_2 nanoparticles is similar. Ramírez Reina et al. [14,113] performed an extensive study over the deposition of bare or transition metal-doped Au/CeO_2 catalyst over alumina. On the other hand, Escamilla-Perea et al. [114] proposed the use of SBA-15, and Hernandez et al. [115] the use of wormhole hexagonal mesoporous silica. The neutral surfactant templating route was used to prepare the latter, and its modification with cerium oxide was performed either by direct synthesis or by impregnation methods. Gold was finally deposited via deposition–precipitation.

Carabineiro and coworkers have synthesized cerium oxides by an exotemplating procedure [116], using activated carbon or carbon xerogel as templates. The resulting Au/CeO_2 catalyst was produced via the double impregnation method (a modification of the deposition–precipitation method). Furthermore, they have applied the solvothermal method for obtaining ultrafine cubic CeO_2, using methanol as a solvent and studying other variables during the synthesis [117]. The obtained cerium oxides were used as supports for the deposition of gold through the double impregnation method and these materials were compared with a reference gold catalyst synthesized with a commercial ceria. Although the use of the solvothermal methodology resulted in the slight decrease in the catalytic performance of the gold catalysts during the CO oxidation reaction due to the sintering of the gold nanoparticles, for these materials, a superior contribution of the oxidic gold species was observed; for the reference catalyst, the gold species were in the metallic state. This result remarks that the structural properties of the materials are strongly influenced by the different variables involved in the synthesis process. In this sense, Carabineiro et al. [118] have also studied the effect of the nature of the gold precursors used for obtaining Au/CeO_2 catalysts, observing the promotion of gold sintering when chlorine remains in the solids.

Moreover, Liu et al. [119] proposed three-dimensional ordered macroporous (3DOM) Au/CeO_2–Co_3O_4 system with well-defined macroporous skeleton and mesoporous walls created via a precursor thermal decomposition-assisted colloidal crystal templating method. They found long-term stability of the material under CO–PROX reaction conditions and attributed it to the 3DOM interconnected mesoporous wall structure, which can efficiently transfer reactant species.

Equal or even more variation of the synthetic methods concerning ceria can be found in the literature. The morphology-dependent catalysis reported in the case of ceria-based systems excites a variety of publications dealing with the controlled synthesis and self-assembling of the ceria structures [120,121]. As the Au/CeO_2 interaction is of paramount importance in order to design and fabricate well performing catalytic materials, the control of the ceria morphology, and the gold particle size will result in a fine control of Au/CeO_2 interface. Huang et al. [122] compare the catalytic properties of Au nanoclusters deposited on one-dimensional CeO_2 (1-D) nanorods to conventional nanoparticulated CeO_2. This study reveals that the predominantly exposed (100)/(110) surface of the ceria nanorod structures notably affects Au dispersion, which in turn leads to a higher redox activity, catalyst reducibility, and superior activity in the CO oxidation reaction. The effect of the ceria

morphology on the catalytic activity of gold-based catalyst in the CO oxidation reaction was also reported [123]. Uniformly distributed crystalline nanorods, nanocubes, and nanopolyhedra of ceria were prepared via a hydrothermal method, and Au was deposited via colloidal one. Ceria materials exposing other than (100) faces were more active in the oxidation reaction. The Au/CeO_2 nanorods (110 + 100) and Au/CeO_2 nanopolyhedra (111 + 100) showed higher activity than Au nanocube (100) catalysts. A one-step hydrochloric acid-assisted solvothermal method for the preparation of well-dispersed CeO_2 hollow nanospheres with high surface area and its decoration by colloidal Au nanoparticles were reported by Liu et al. [124]. According to the authors, this method leads to the existence of different Au species, both metallic and positively charged, which strengthened the interface interactions with the support. Zhu et al. [125] proposed a method for in situ growth of Au/CeO_2 core-shell nanoparticles and CeO_2 nanotubes by mixing gold and ceria precursors. The particularity of this method is that the used ceria precursor was already preformed $Ce(OH)CO_3$ nanorods. The formation of the Au/CeO_2 core-shell nanocomposite was obtained through an interfacial oxidation–reduction reaction between $HAuCl_4$ and $Ce(OH)CO_3$, where Au(III) was reduced to Au(0) by Ce(III) that was oxidized to Ce(IV). A final hydrolysis step generates CeO_2 nanoparticles. The advantage of this synthetic strategy was reported to be the independence of the method of foreign reducing agents and surface modifications. Hierarchical structures based on gold nanoparticles embedded into hollow ceria spheres and a mesoporous silica layer were proposed by Zhang et al. [126]. Compared with the $CeO_2/Au/SiO_2$ catalyst, the obtained hierarchical composite exhibits superior catalytic activity in the hydrogenation of 4-nitrophenol at room temperature, behavior assigned to the synergistic effect between the hollow structure and the mesoporous shell.

As seen from the above-mentioned examples, more and more complex structures are proposed every day. Nevertheless, no matter what the employed method of ceria preparation or gold deposition is, only a fine control of size and morphology of both components is required for their successful application in a variety of reactions.

3. Characterization of Au/CeO_2 Catalysts Involved in Oxidation Reactions

Since the discovery in 1987 by Haruta and coworkers of the catalytic activity of very small gold particles (<5 nm) supported on different oxides in the CO oxidation, even at temperatures below room temperature [3], a huge number of studies have been devoted to the application of gold nanoparticles, not only for CO oxidation but also for different oxidation reactions. There are evidences that gold may be involved in the adsorption or the activation of the reactants during the oxidation reactions, and this strongly depends on its interaction with the support by means of electronic transfer, which is also dependent of the particle size and physical structure of the gold clusters [60]. Chen and Goodman [6] have demonstrated that the CO oxidation ability increases until a maximum value by decreasing the gold nanoparticles to 3 nm; below this size, the CO conversion decreases. These results are consistent with several works in which the higher catalytic activity in CO oxidation reactions is achieved by means of depositing gold on reducible supports [127,128].

Generally, excellent catalytic properties in the oxidation reactions [15,28,129–135] and WGS reaction [136–139] can be obtained by combining gold with bare ceria or by using modified ceria oxides. Upon ceria modification, the enhancement of some structural properties has resulted in a relevant improvement of the catalytic activity. The easiness of Ce^{4+} cations to Ce^{3+} reducibility results in the creation of oxygen vacancies and allows considerable mobility of the surface oxide ions of the ceria lattice [60]. The determinant role of ceria's punctual defects in oxidation reactions has been widely proven. In fact, this material is considered as an active support when employed to prepare catalysts for oxidation reactions.

Moreover, the dispersion of gold over support surfaces has been shown to be dependent on the oxygen vacancies population within the oxide [11,15,17,20,51,57,127,140–144]. Rodríguez et al. [139] evidenced via Scanning Tunneling Microscopy (STM) the presence of oxygen vacancies in a model catalyst formed by CeO_2 nanoparticles dispersed on the (111) surface of a gold single crystals.

Similarly, Au nanoparticles deposited via Physical Vapor Deposition (PVD) on CeO_2 (111) were also studied via STM. This study reveals that gold preferentially nucleates on surface defects. Moreover, the generation-annihilation of defects during the CO oxidation reaction is intimately connected with the reactivity of ceria surfaces [145]. This dynamic of gold clusters on the ceria surface has been corroborated by Density Functional Theory (DFT) calculations on model systems. These calculations emphasize the role of surface oxygen vacancies on the sintering-breakdown of gold nanoparticles as a function of temperature and reaction atmosphere [135]. Gold nucleation on Eu-modified ceria surface vacancies has been assessed by Raman spectroscopy and X-ray diffraction (XRD). In this study, Hernández et al. [20] show that oxygen vacancy concentration and gold dispersion is a function of the employed atmosphere and temperature. The redox processes occurring at the ceria surface during reaction determines the gold reversible sintering-breakdown processes. Moreover, this reversible transformation is strongly affected by the hydroxylation of the reducible oxide surface that, at high temperatures, is involved in the re-oxidation of the cerium sites in a mechanism that implies the competition of hydroxyl groups and gold atoms for oxygen surface vacancies [25]. DFT calculations of the role of water on CO oxidation over Au/TiO_2 catalysts support this H_2O–Au competition for surface oxygen vacancies [12,18].

Consequently, the catalytic performance of this sort of material during the oxidation reactions is closely related to the interaction between gold and these punctual defects. This has driven numerous efforts for understanding the behavior of this kind of defects in order to pretend control their influence on the particle size distribution of gold. Nevertheless, surprisingly, there is not a general agreement on the nature of the active sites in this kind of catalyst during oxidation reactions. This is why different conclusions about the chemical nature of the more active gold species may be found in the literature [146], and evidences of a determinant catalytic role of Au^+ species [34,147] or even Au^{3+} species [128] have been presented.

For instance, Casalleto et al. [148] observed the presence of Au^0, Au^+, and Au^{3+} species in Au/CeO_2 catalysts by means of X-ray photoelectron spectroscopy (XPS) analyses and proposed Au^+ species as effective in promoting CO oxidation at low temperature. Despite this, Corma et al. [128] presented spectroscopic evidences of oxygen supply during CO oxidation catalyzed by gold supported on nanocrystalline ceria. The authors established a correlation (Figure 2) between the specific rate for CO oxidation and the ratio between the intensities of the infrared signals associated with the adsorption of CO over Au^{3+} (band at 2148 cm^{-1} representing Au^{3+}–CO) and Au^0 species (band at 2014 cm^{-1} representing Au^0–CO).

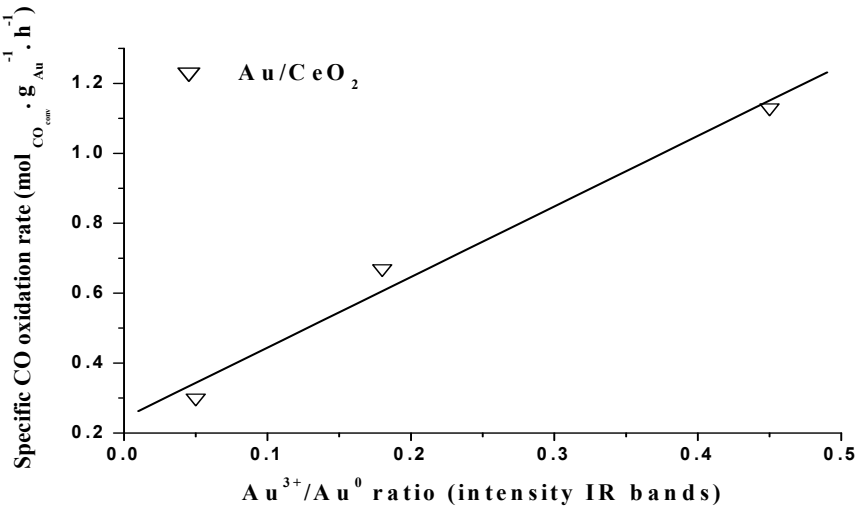

Figure 2. Correlation between Au^{3+}/Au^0 species and specific rate for CO oxidation catalyzed by gold supported on nanocrystalline ceria. Adapted from Guzman et al. [128].

The authors also proposed that nanocrystalline ceria supplies reactive oxygen in the form of surface superoxide η^1 species and peroxide adspecies at a one-electron defect site to the supported active gold species to oxidize CO. The presence of the cationic species of gold was confirmed by means of XPS measurements, and the presence of superoxide and peroxide species on ceria throughout Raman spectroscopy. The formation of peroxide species upon oxygen adsorption on electron-rich support vacancies has also been proposed for other Au catalysts [21].

Rodríguez et al. [149] studied the decomposition of SO_2 over Au/CeO_2 (111) and AuO_x/CeO_2 species, analyzing the adsorption of this molecule over their surfaces by means of synchrotron-based high-resolution photoemission. These authors observed a complete decomposition of SO_2 achieved only after the introduction of oxygen in the ceria support. Therefore, they associated the active sites of the $[Au + Au_x]/CeO_2$ system to pure gold nanoparticles in contact with oxygen vacancies, demonstrating the activating role of such defects over the clusters of noble metal.

All of these models only coincide on the importance of the Au/CeO_2 interface for achieving excellent catalytic activity of those systems.

The relevance of the interaction between gold and oxygen vacancies has driven other interesting studies on the structural properties of this kind of catalyst: These properties can be resumed in different categories such as textural properties, reducibility, oxygen mobility, oxygen storage capacity (OSC), and morphology, among others. Experimental evidences have shown that all of these properties may be modulated by modifying the synthesis procedure of Au/CeO_2 systems. For instance, Si and Flytzani-Stephanopoulos in order to establish the possible effects of the preferential exposition of some crystal-planes of the ceria surface on the WGS reaction studied synthesis procedures allowing for the obtainment of morphology-controlled ceria nanoparticles [138]. Figure 3 shows micrographs of the obtained ceria nanoparticles morphologies and the corresponding catalytic performance of 1% Au/CeO_2 catalysts. Rod-like ceria nanoparticles enclosed by (110) and (100) planes resulted in higher activity for the WGS reaction, demonstrating the strong influence of ceria morphology on Au/CeO_2 catalytic behavior.

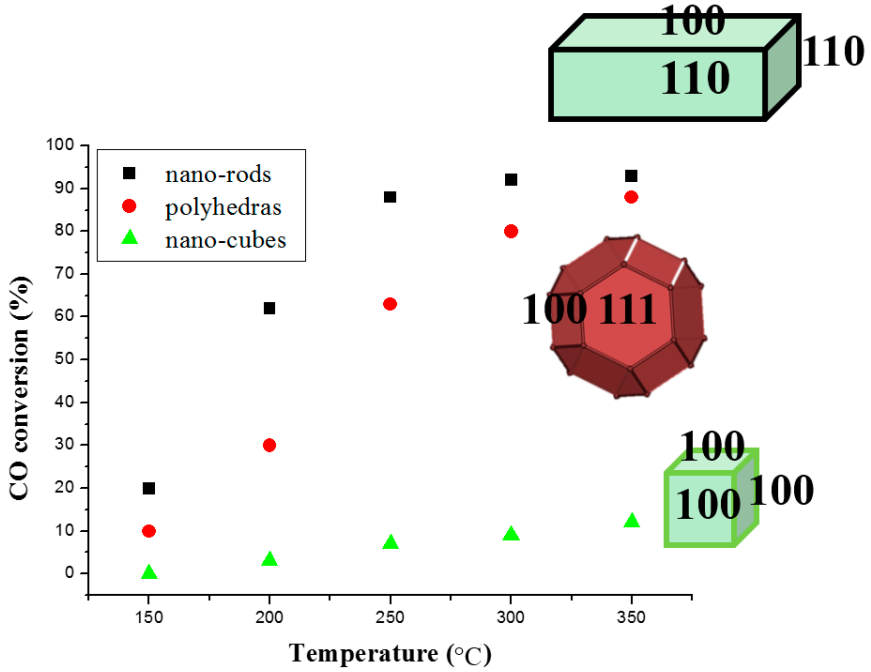

Figure 3. Gold nanocluster for the water gas shift (WGS) reaction: Different morphologies of the obtained gold nanoclusters and their Catalytic activity during the WGS reaction. Adapted from Si et al. [138].

Concerning the textural properties, it seems that gold nanoparticles deposition over ceria or doped ceria systems does not produce dramatic alterations. Only a slight decrease in Brunauer Emmet Teller (BET)-specific surface area can be observed, often attributed to the calcination process after gold deposition that may promote surface area drop. Higher stability of the textural properties and, in some cases, an increase in the specific surface area is achieved in doped ceria systems. This effect is more frequently associated to the inclusion of doping agents rather to the presence of gold.

Nevertheless, not all heteroatoms modify the cerium oxide in the same way. For instance doping ceria with Zr, Zn, and Fe results in supports for gold catalysts with different properties [51]. Solid solution formation was achieved only in the case of Zr and Fe doping, whereas the use of Zn resulted in ceria and zinc oxide segregation. Only the introduction of Zr into the framework of ceria resulted in textural property promotion (higher BET surface area). After gold deposition, no further differences in the BET area occurred; however, the average pore size increased. This phenomenon has been also previously reported by Domínguez et al. [150] over Au/Al_2O_3 and Au/CeO_2 catalysts deposited on reticulated ceramic foams issued from stainless steel wastes and employed for the 2-propanol oxidation. In this work, the change of the pore structure upon gold particles incorporation was associated with the enlargement of the pores by gold, as proposed previously by Somorjai et al. [151]. According to this, the insertion of gold nanoparticles may modify the porous structure of the supports, including ceria and doped ceria, by increasing their pore sizes.

As for the reducibility studies, they are usually carried out by means of temperature programmed reduction experiments (TPR) using H_2. The temperature of reduction of ceria or doped ceria systems is considerably decreased in the presence of gold [60], especially the reduction of the surface Ce^{4+} cations, promoted by the existence of close contact between oxide and noble metal nanoparticles [152].

Closely related to the reducibility feature of Au/CeO_2 systems is their OSC. According to Duprez et al. [153], Ce-based oxides with cationic valences and oxygen vacancies may be considered as materials with high OSC. These properties allow for the storage of active oxygen species (O^{2-}, superoxide, etc.) in O_2 excess and their release when the partial pressure of oxygen decreases. The experimental procedure for OSC measurements implies the use of reductant molecule, often CO and less H_2 [153]. According to Yao and Yu Yao [154], the CO_2 produced during the first CO pulse allows for the calculation of the OSC, whereas the total amount of CO_2 formed after several CO pulses gives the complete oxygen storage capacity of the material (OSCC).

Fonseca et al. [155] studied Au/CeO_2, CuO_x/CeO_2, and $Au–CuO_x/CeO_2$ catalysts for the CO–PROX reaction and observed by means of OSC measurements that about one monolayer of ceria can be reduced at 400 °C. The surface reducibility of the systems with gold (Au/CeO_2 and $Au–CuO_x/CeO_2$) is always superior at lower temperatures compared with the initial supports (CeO_2, CuO_x/CeO_2). This seems to be closely related to their catalytic behavior, with all gold-based materials clearly superior in the CO oxidation at low temperatures. Furthermore, a cooperative gold–copper effect was established for the $Au–CuO_x/CeO_2$ resulting in moderate and totally reversible inhibition by CO_2 presence and absence of inhibition by H_2O.

The OSC over gold-based catalysts prepared with doped ceria systems as supports ($Au/M–CeO_2/Al_2O_3$; M = Fe, Cu, and Zn) has been also studied by Reina et al. [142]. In this case, like in all previously reported, the enhancement of the OSC by the presence of noble metal was observed at a low temperature (150 °C). The authors described the role of the noble metal as a "channel", allowing the oxygen migration from the gaseous phase to the structure or in the opposite way via the storage of oxygen species in the framework of the support.

4. Au/CeO_2 Catalysts: Structure and Oxidation Activity

4.1. Oxidation Reactions Catalyzed by Au/CeO_2

A well-known property of bulk metallic gold is its high inertness and non-changing character being ideal for jewelry purposes. Its low chemical and catalytic activity converts gold in the least

reactive transition metal, often referred also as "coinage metal" [70,146,156]. However, gold becomes extremely active when subdivided into nanoscale (usually less than 5 nm) and dispersed over an adequate metal oxide or over activated carbon supports [15,29,64,71,138,157]. Among the different options, ceria results frequently in an optimum choice as support for gold nanoparticles. Due to its excellent redox properties, ceria is probably the most extended support employed in oxidation catalysis, and Au/CeO_2 combinations result in a perfect synergy. Here, the attention is driven to a number of reactions in which Au/CeO_2-based catalysts have an outstanding behavior.

4.2. CO Oxidation

The activity of gold-based catalysts towards CO oxidation is known to be sensitive to (i) the preparation method; (ii) the nature of the supports; (iii) the size of the gold particles; (iv) the pre-treatment conditions; and (v) the gold–support interactions [10]. Among all the support choice is of primordial importance. The support usually plays multiple roles, such as mechanical functionality, i.e., to disperse and stabilize the supported nanoparticles against agglomeration and at the same time it could participate in the catalytic process.

Conventionally, the supports for CO oxidation can be classified depending on their reducibility or ability to supply reactive oxygen: reducible materials such as CeO_2, Fe_2O_3, CoO_x, and non-reducible supports such as MgO and Al_2O_3. Currently, gold supported on a reducible transition metal oxide always exhibits better activity for CO oxidation than gold supported on non-reducible oxides [6,158]. However, non-reducible materials with electron-rich oxygen vacancies may also enhance the catalytic activity of gold by activating gaseous oxygen [16,21]. Ceria, due to its chemical properties, has become one of the most promising supports for oxidation reactions and has been broadly studied [7–10,15,17,20,26,28,51,57,129,143,159–161]. The relevance of cerium oxide, as a support for gold nanoparticles, is mainly based on its high oxygen storage capacity resulting from oxygen mobility in its lattice [47]. The latter is directly correlated to the creation, stabilization, and diffusion of oxygen vacancies, especially on oxide surfaces, due to the reversible redox behavior of the Ce^{4+}/Ce^{3+} couple and leading to the formation of non-stoichiometric oxides CeO_{2-x} $(0 < x < 0.5)$. The concentration of these structural defects is usually correlated with the catalytic activity in CO elimination reactions [51,127,146,162–165]. In addition, these defects may act also as activation points of the CO and O_2 molecules, facilitating the reaction. Indeed, the participation of ceria in the reaction mechanism is vital since the main criticism towards CO oxidation mechanisms involving only Au atoms is related to the poor capacity of gold for oxygen chemisorption and activation [60]. Figure 4 shows a simplified reaction mechanism for the CO oxidation over Au/CeO_2. The rapid Ce^{4+}/Ce^{3+} interconversion leads to the generation of oxygen vacancies (Equation (1)), where O_2 can be chemisorbed (Equation (2)). In parallel, carbon monoxide sits on metallic gold particles (Equation (3)), leading to adsorbed CO that would further react on the metal/oxide interface with O activated in the support vacancy producing the final CO_2 (Equation (4)).

$$(CeO_2) \rightarrow \frac{1}{2}O_2 \uparrow + V_O^{\bullet\bullet} + 2e' \rightarrow \frac{1}{2}O_2 \uparrow + V_O^{\bullet\bullet} + 2Ce'_{Ce}; \quad (1)$$

$$V_O^{\bullet\bullet} + O_2 \rightarrow V_O^{\bullet\bullet} - O_{2(ads)}; \quad (2)$$

$$Au + CO_{(g)} \rightarrow Au - CO_{(ads)}; \quad (3)$$

$$Au - CO_{(ads)} + V_O^{\bullet\bullet} - O_{2(ads)} \rightarrow CO_2 \uparrow + Au + V_O^{\bullet\bullet}. \quad (4)$$

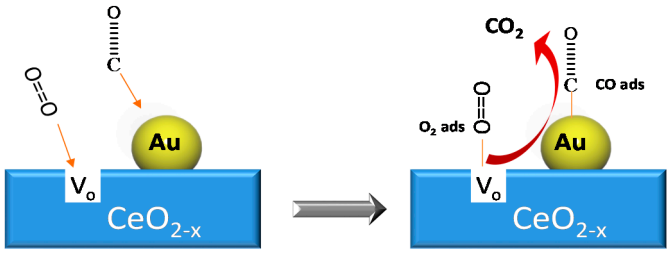

Figure 4. Simplified CO oxidation mechanism in a model Au/CeO_2 system. Oxygen vacancies of ceria on the Au/CeO_2 contact perimeter can chemisorb gaseous oxygen (O==O → V_o) producing activated oxygen atoms able to react with CO molecules adsorbed on Au particles (C==O → Au) to generate gaseous CO_2 and new oxygen vacancies.

Some authors have suggested that the presence of gold clusters weakens the oxygen species bonding on CeO_2 lattice, thus facilitating the formation of more reactive species [34,136]. In some cases, these reactive sites can participate in the reaction mechanism by creating activated species directly from the reactants mixture (e.g., peroxi-like and superoxi-like species), potentiating the oxidation reactions [166–169]. Guzman et al. [170] clearly demonstrated the role of these oxygen activated species in the CO oxidation process using in situ Raman spectroscopy. They obtained Raman spectra of gold supported on nanocrystalline ceria before and during the CO oxidation test, detecting bands at 1123 and 966 cm^{-1} ascribed to superoxide and peroxide species, respectively [171]. These bands virtually disappear during CO oxidation, indicating the direct participation of these oxygen species in the reaction. In this study, it is also stated that the formation of defect sites on nanocrystalline ceria is promoted by the gold presence underlying the importance of the Au/CeO_2 contact and their synergistic effect [170]. Figure 5 schematizes the CO oxidation process picturing the direct participation of reactive oxygen species in the process. This synergistic effect has also been demonstrated for ZnO-doped CeO_2 systems where the band at 1127 cm^{-1} ascribed to superoxide-like species has been observed by FTIR [172].

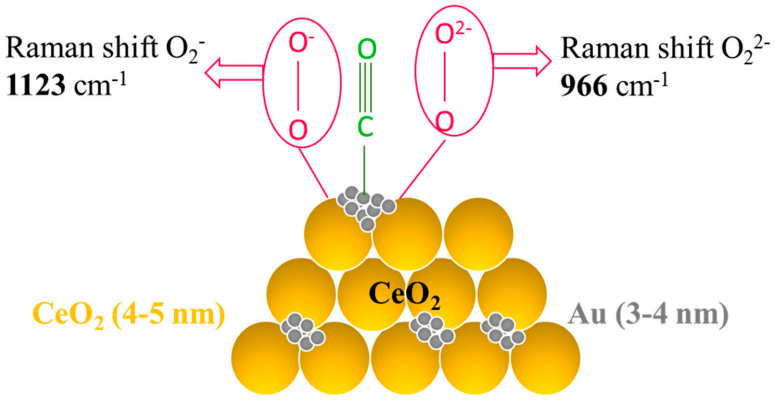

Figure 5. Schematic representation of CO oxidation catalyzed by gold on nanocrystalline reflecting the role of oxygen reactive species. (CeO_2 yellow, Au grey. The position of the characteristic Raman bands of superoxide (O_2^-, 1123 cm^{-1}) and peroxide (O_2^{2-}, 966 cm^{-1}) species are shown). Adapted from Guzman et al. [170].

Given the importance of the oxygen defects in ceria to achieve high performances in CO oxidation, there has been a research trend in the last decade aiming to potentiate oxygen vacancy formation on ceria lattice. The O^{2-} removal from the oxide surface or oxide lattice can be achieved via several methods such as thermal treatments [173], electron irradiation [174], X-rays exposition [175], or chemical reduction [51]. However, for catalytic applications, the most popular strategy is to

dope ceria with lower valence metallic cations [20,176–178]. The formation of oxygen vacancies in CeO_2–MO_x support is directly related to the formation of a Ce–M solid solution. The dopant ions with electronegativity and ionic radius close to those of cerium cations are considered the most appropriate modifiers of ceria structural and chemical properties. The presence of these dopants can provoke structural distortions such as ceria lattice contraction, thus favoring the formation of oxygen vacancies by mechanical stress.

Extensive research carried in our laboratory show the positive effect of a number of dopants including Eu [20,57], Zn [15,17,51], Fe [51,53,174], Cu [37,160], Zr [11,51,179,180], Gd [56], Ni [143], Cr [143], and Co [14], which potentiate ceria defect chemistry resulting in highly effective catalysts for oxidation reactions. Several situations may be envisaged as a function of the dopant cation. In the case of solid solutions formation on doping ceria with aliovalent cations, several mechanisms may occur for compensating the differences in the formal charge of cations. All possible compensation mechanisms are summarized in the following defect equations:

$$x\mathrm{M_2O_3(CeO_2)} \rightarrow 2x\mathrm{M'_{Ce}} + x\mathrm{V_O^{\bullet\bullet}} + 3x\mathrm{O_O^x}; \quad (5)$$

$$x\mathrm{M_2O_3(CeO_2)} \rightarrow \frac{x}{2}\mathrm{M_i^{\bullet\bullet\bullet}} + \frac{3x}{2}\mathrm{M'_{Ce}} + 3x\mathrm{O_O^x}; \quad (6)$$

$$x\mathrm{M_2O_3(CeO_2)} \rightarrow 2x\mathrm{M'_{Ce}} + \frac{x}{2}\mathrm{Ce_i^{4\bullet}} + 3x\mathrm{O_O^x}; \quad (7)$$

$$x\mathrm{MO(CeO_2)} \rightarrow x\mathrm{M''_{Ce}} + x\mathrm{V_O^{\bullet\bullet}} + x\mathrm{O_O^x}. \quad (8)$$

The vacancy compensation mechanism is schematized in Equation (5). In this situation, two M^{3+} cations replace two Ce^{4+}, leading to the formation of one oxygen defect. The dopant interstitial compensation, Equation (6), and the cerium interstitial Equation (7) mechanisms do not result in vacancy formation. Furthermore, for the case of divalent cations, Equation (8), one M^{2+} ion replaces one Ce^{4+} species, also resulting in one oxygen defect. In particular, the interstitial compensation mechanism and oxygen vacancies creation using divalent cation are very frequent. Empirical calculations carried out for M^{3+} cations show that the oxygen vacancy compensation mechanism is undoubtedly the preferred route, especially for large dopants cations (radius > 0.8 Å) [48]. Solid solutions with isovalent cations result in a slightly different situation. For example, the use of Zr^{4+} as a dopant potentiates the creation of oxygen vacancies, but this effect is mainly due to the distortion of ceria lattice and mechanical stresses induced by the differences in ionic radii between cerium and zirconium [11,51]. However, even if solid solutions cannot be formed, as in the case of Zn [15,17,51], the formation of oxygen vacancies under CO atmosphere is enhanced by the close contact between ZnO crystallites and CeO_2 nanoparticles [172] according to the model summarized in Equations (9)–(14):

$$x\mathrm{ZnO} \xrightarrow{\mathrm{CO}} x\mathrm{V_O^{2\bullet}(ZnO)} + x\mathrm{Zn_{Zn}^x} - \mathrm{CO_2(ads)}; \quad (9)$$

$$\mathrm{Zn_{Zn}^x - CO_2(ads)} \rightarrow \mathrm{Zn_{Zn}^x} + \mathrm{CO_2}\uparrow; \quad (10)$$

$$\mathrm{V_O^{2\bullet}(ZnO)} + \mathrm{O_O^x(CeO_2)} \rightarrow \mathrm{V_O^{2\bullet}(CeO_2)} + \mathrm{O_O^x(ZnO)}; \quad (11)$$

$$\mathrm{V_O^{2\bullet}(CeO_2)} + \mathrm{Ce'_{Ce}} \rightarrow \mathrm{Ce_{Ce}^x} + \mathrm{V_O^{\bullet}(CeO_2)}; \quad (12)$$

$$\mathrm{O_2} + \mathrm{V_O^{\bullet}(CeO_2)} \rightarrow \mathrm{V_O^{2\bullet}(CeO_2) - O_2^-(ads)}; \quad (13)$$

$$\mathrm{Ce_{Ce}^x} + \mathrm{V_O^{2\bullet}(CeO_2) - O_2^-(ads)} \xrightarrow{\mathrm{CO}} \mathrm{Ce'_{Ce} - CO_3^{2-}(ads)} + \mathrm{V_O^{\bullet}(CeO_2)}. \quad (14)$$

In this model, the limiting reaction is the formation of oxygen vacancies in ZnO. This ZnO_{1-x} phase acts as an oxygen vacancy generator in the ceria phase. These vacancies are the active sites for activating oxygen as superoxide ions.

Figure 6 provides an example of CO oxidation activity improvement achieved when Fe or Zn are employed as CeO_2 dopants. The addition of tiny amounts of Zn and Fe (1 and 2 wt %) notably boost

the CO oxidation activity of the Au/CeO_2-based materials. The results are especially impressive given the fact that all doped catalysts reached full CO conversion at sub-ambient temperatures, while the unmodified $Au/CeO_2/Al_2O_3$ achieved complete CO abatement at around 40 °C. In this specific case, the main difference between Fe and Zn as ceria promoters is that, while Fe^{3+} cations can replace Ce^{4+} forming a Ce–Fe solid solution [36,48], Zn^{2+} does not enter into ceria lattice. However, in both situations, a higher population of oxygen vacancies is identified. The immediate consequence of Ce–Fe solution is the formation of oxygen vacancies to balance the lattice charges upon substitution. Zn instead promotes surface ceria reducibility, generating oxygen defects at the $ZnO–CeO_2$ interface as described above [14].

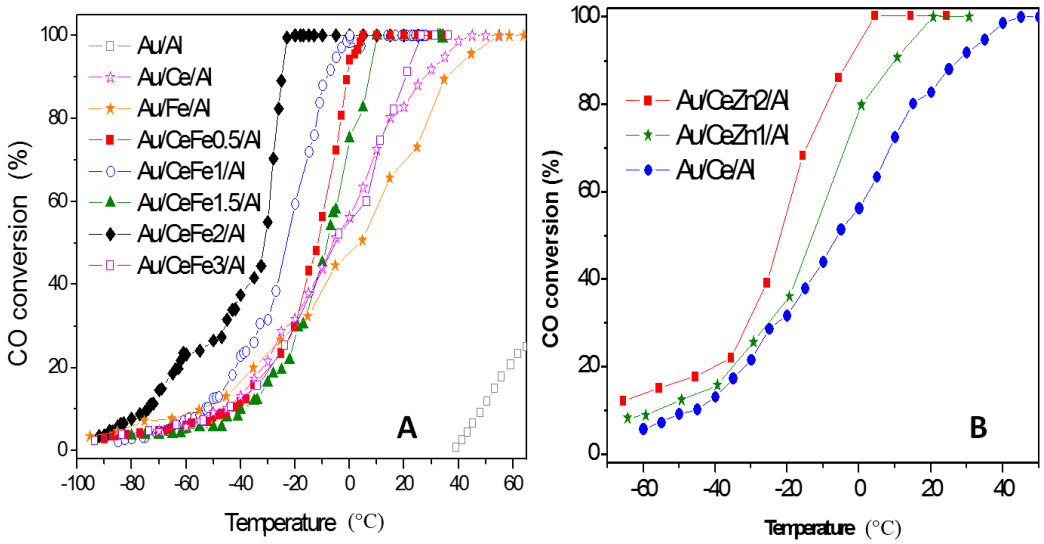

Figure 6. CO oxidation activity of Fe- and Zn-doped $Au/CeO_2/Al_2O_3$ catalysts (reaction conditions: 3.4% CO and 21% O_2, balanced in helium and Weight Hourly Space Velocity, WHSV, of 31.5 $Lg(cat)^{-1}\cdot h^{-1}$). (**A**) Fe-doped $Au/CeO_2/Al_2O_3$; (**B**) Zn-doped $Au/CeO_2/Al_2O_3$. Reproduced with permission from [113]. Copyright Ramirez Reina, Ivanova, Centeno and Odriozola, 2013.

Despite the encouraging results reported for Au supported on promoted ceria, there have been some examples where the use of a dopant does not benefit the activity and could lead to detrimental results instead. For instance, in a recent paper from Reddy's group, some potential ceria promoters such as Fe^{3+}, Zr^{4+}, and La^{3+} for CO oxidation were analyzed [178]. Fe and especially Zr greatly boosted the CO oxidation capacity of the original Au/CeO_2 catalysts, while La shifted the light off curve towards higher temperatures. Furthermore, the La-doped material was not able to reach a full conversion in the studied temperature range. Apparently, while Zr and Fe favor the formation of ceria oxygen vacancies and improve ceria textural properties, the La incorporation caused a negative effect due to the presence of carbonate species blocking the active sites essential for CO oxidation. Thermogravimetric Analyses (TGA) revealed that the carbonates species formed on La-doped ceria are stable and remained anchored on the catalyst surface even at high temperatures. According to these authors, further tuning of the acidity of the support seems to be a sensible way to control carbonates formation [178].

In summary, Au/CeO_2-based catalysts represent an excellent option for direct oxidation of carbon monoxide in contaminated atmospheres with potential application in environmental catalysis. A number of factors can influence the catalytic properties of this type of material, such as gold particle size, preparation method, and Au/CeO_2 contact. Most of these parameters are broadly discussed in the literature and are not the subject of this section. However, there is general agreement on the important role played by ceria. With all other factors optimized (nanogold particle size, metallic dispersion, etc.), highly effective CO oxidation catalysts can be produced only when ceria electronic properties and

defect concentration is tailored with an adequate dopant. Vast efforts has been made in recent years aiming to achieve an optimum performance, but there is still some room for further improvements.

4.3. WGS

As for the CO oxidation, the most popular supports for gold nanoparticles in WGS reactions are CeO_2-, TiO_2-, Al_2O_3-, Fe_2O_3-, ZrO_2-, and carbon-based materials, and combinations thereof [146]. However, ceria has taken the edge over all other supports and has recently become the most used material in gold-catalyzed WGS reactions. Figure 7 reflects this issue. Most of the works carried out in the WGS reaction using gold-based catalysts have included ceria as a part of the catalytic formulation.

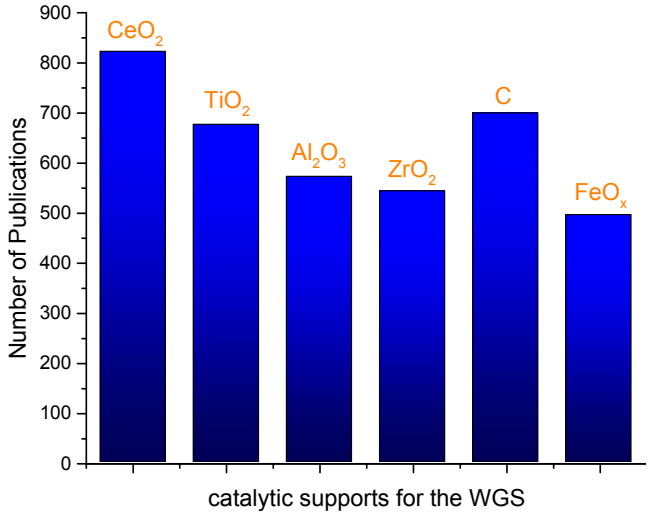

Figure 7. Number of published papers available in Scopus Scholar data base using "gold catalysts" and "WGS" and "CeO_2" or "TiO_2" or "ZrO_2" "Carbon supports" or "Al_2O_3" or "Fe_2O_3" as search strings (September 2016).

The success of CeO_2 in the WGS is mainly due to the combination of an elevated OSC and a high ability to shift easily between reduced and oxidized states (Ce^{3+}/Ce^{4+}). A fundamental study of the reaction provides a deeper understanding of the benefits of ceria in this particular process. For instance, a theoretical investigation applying DFT methods to an ideal Au/CeO_2 system clearly illustrated that the water dissociation step into OH and H fragments is the rate limiting step for the WGS [146]. Figure 8 shows results from Rodriguez's lab clarifying these aspects. Au (111) or Au nanoparticles have poor catalytic performance due to their inability to carry out the O–H bonds breaking in the water dissociation process ($H_2O \rightarrow OH + H$). As indicated in Figure 8A, the biggest energy gap for gold is associated to this water activation transition state. However, the addition of ceria greatly improves the hydrogen production. The relatively large energetic barrier can be overcome by using ceria and specifically ceria oxygen vacancies as nucleation points to activate water. For comparison other metals, as for example Cu, can perform the water splitting by itself without support assistance since they present a much smaller energy barrier (Figure 8B).

It is worth mentioning that a perfect (111) CeO_2 surface is not able to dissociate water either. The water splitting ability exists only when O vacancies are present [146].

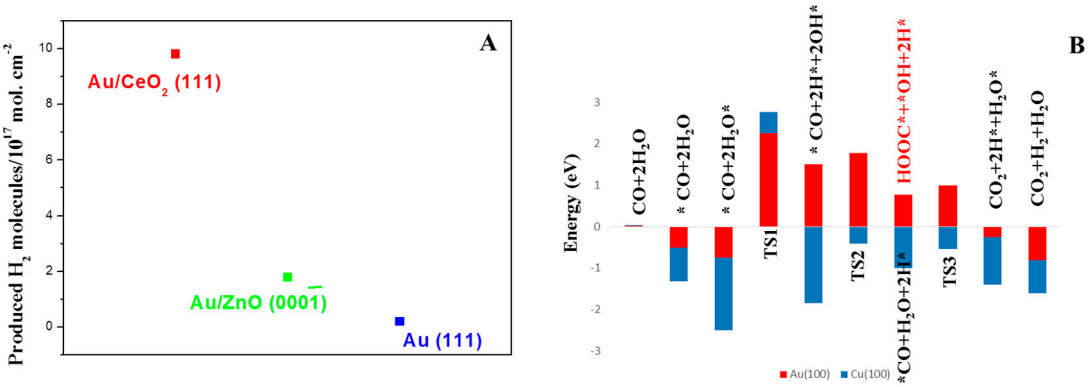

Figure 8. (**A**) Catalytic activity of model WGS catalysts; (**B**) WGS reaction energy profile over Au (100) and Cu (100). Adapted from Rodriguez [146].

It is well accepted that the WGS reaction on an Au/CeO_2 catalyst proceeds as follows: CO is absorbed on Au sites, water splitting occurs on oxygen vacancies of the support, and the subsequent reaction takes place on the metal-oxide interface [165]. On these premises, the design of efficient catalysts for the WGS reactions involves the dispersion of very small gold nanoparticles on a highly defective ceria carrier.

The importance of oxygen vacancies and Au/CeO_2 synergy to achieve high performance is inherently imposed by the reaction mechanism. Conventionally, two main mechanism are proposed for the WGS: (i) the so-called redox mechanism (or surface mechanism), where CO adsorbs on gold particles and reacts with oxygen from the support, which, in turn, is reoxidized by water; and (ii) the associative mechanism, also called formate mechanism, where formate-like species are generated from the interaction of CO with OH groups of the support. The decomposition of these intermediates yields to the reaction products, CO_2 and H_2 [32]. Irrespectively of the mechanism ruling the process, the participation of both gold nanoparticles and ceria acting synergistically is fundamental. Figure 9 schematizes the redox mechanism reflecting the indispensable role played by the mobile oxygen from ceria and ceria oxygen defects.

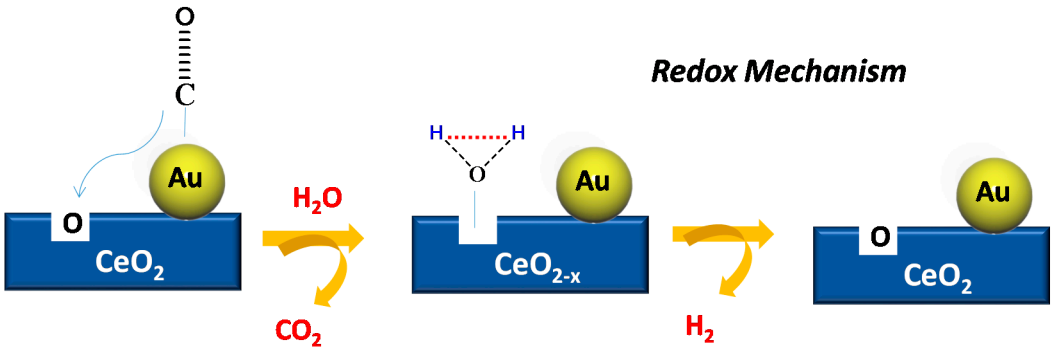

Figure 9. Simplified WGS redox mechanism for a model Au/CeO_2 catalyst.

In this context, intensive research has been carried out aiming to potentiate ceria oxygen mobility and oxygen vacancies population. Similar to the CO oxidation, the most extended strategy to enhance Au/CeO_2 performance is the use of promoters. Rare earth metals are a common option and, when added to ceria, provide improved thermal stability and increased activity [181]. Wang et al. [182] investigated a ceria/zirconia catalyst doped with rare earth metals (La, Nd, Pr, Sm, and Y) and found that all dopants increased activity and selectivity, with La, Nd, and Pr performing best. The results with lanthanum as a dopant of ceria are particularly interesting [183]. Liang et al. reported WGS activity of

Au-supported $La_xCe_{1-x}O_y$ nanorods (x = 0–0.5) with a uniform aspect ratio. They established that the reducibility of $La_xCe_{1-x}O_y$ nanorods is determined by the preferential exposure of highly active (110) planes and by the La-to-Ce ratio. The La doping was found to act as an inhibitor of $La_xCe_{1-x}O_y$ nanorods growth along the [110] direction and resulting in preferential exposure of (110) crystal planes for CeO_2 nanorods, a lower reduction temperature, and an increased number of reducible sites in the WGS reaction temperature range. Fu et al. [184] reported as well an enhanced activity for Au/CeO_2-based catalysts doped with lanthanum and gadolinium.

The only serious drawback of these systems is its stability issue and activity drop due to the formation of cerium/lanthanum hydroxycarbonate in shutdown conditions. Some authors have dealt with the carbonate formation problem and suggested that the tendency of ceria to stabilize carbonate on its surface could be inhibited through the addition of another metal, which does not stabilize these species [185]. Vindigni et al. [137] reported that $Ce_{50}Zr_{50}$ and $Ce_{80}Zr_{20}$ mixtures present similar acidities, both being two times higher than that of pure ceria. Therefore, zirconia addition modifies the acid–base properties of the support and less stable carbonate-like species are formed. This feature, along with the presence of high gold dispersion, makes $Au/Ce_{50}Zr_{50}$ the best catalyst in terms of catalytic activity and stability within the studied systems. At the same time, the addition of zirconium has a positive impact on the OSC of ceria [186]. Zirconium facilitates lower-energy bonding between oxygen molecules when compared to pure ceria. These weakly bonded oxygen molecules allow higher reducibility and thereby higher OSC, which in turns facilitates the WGS reaction [187].

The impact of the OSC in the WGS performance of a series of transition-doped $Au/CeO_2/Al_2O_3$ catalysts was recently addressed [142]. As shown in Figure 10A, all dopants (Cu, Fe, and Zn) sensibly boost the oxygen storage capacity of the reference $Au/CeO_2/Al_2O_3$ catalysts, an effect especially important at the highest studied temperature (350 °C) where the stability of the reaction intermediates is weakened; most likely, the redox mechanism dominates the process. Bearing in mind that the OSC informs about the most reactive and most available oxygen atoms on catalyst surfaces directly involved in the redox process, there must be a direct correlation between OSC and catalytic activities in redox reactions as WGS. Indeed, the catalytic activity Figure 10B follows the same trend as the OSC at high temperature: Fe-doped $Au/CeO_2/Al_2O_3$ > Zn-doped $Au/CeO_2/Al_2O_3$ > Cu-doped $Au/CeO_2/Al_2O_3$ > $Au/CeO_2/Al_2O_3$.

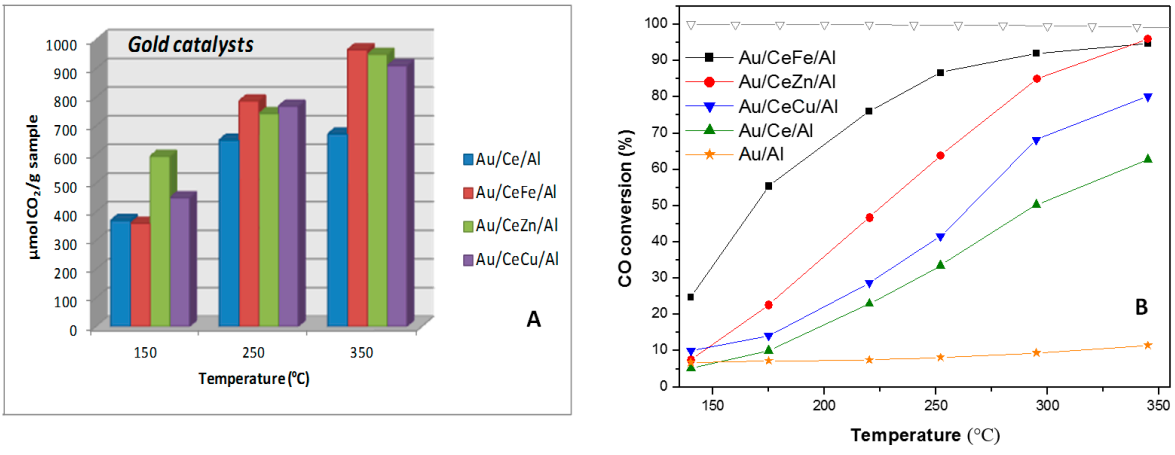

Figure 10. Oxygen storage capacity (OSC) (**A**) and catalytic activity (**B**) of several $Au/CeO_2/Al_2O_3$-doped systems. Reproduced with permission from [142]. Copyright Elsevier, 2015.

Alternatively, instead of modifying ceria support, gold can be promoted by another metal. For instance, Cu [188] and Co [189] were successfully employed to produce highly active $Au–Cu/CeO_2$ and $Au–CoO_x/CeO_2$ for the WGS reaction. In the case of cobalt, the authors conclude that the bimetallic catalysts adsorb more CO molecules, since it could be adsorbed on both cobalt and gold surfaces.

The facilitated CO adsorption together with the improved OSC of cobalt containing catalysts explain the excellent WGS activity [189]. In the case of bimetallic Au–Cu, the addition of Au over CuO/CeO_2 promotes its capacity to release lattice oxygen and makes the oxidation of CO at low temperatures easier [188]. A more exhaustive study regarding bimetallic systems was presented by Juan et al. [190]. It was demonstrated that the addition of Pt, Pd, W, or Ni to Au–ceria provoke a synergistic effect and the resultant bimetallic catalysts are much more active than the parent Au–ceria system, Au–Pt–Ceria being the most active one. The authors expressed the activity in terms of CO fractional conversion and not in normalized specific activities (activity per metal site), since the interactions in the bimetallic catalysts are not sufficiently clear to differentiate between CO adsorption on one metal or another. The total number of metal sites per gram of the catalyst (in mmoles per gram), evaluated via CO chemisorption with the assumption of 1:1 CO to metal site ratio, was 2.7 on Au, 3.8 on Pt, and 2.5 on the Au–Pt sample [190]. Further details of the activity normalization are given in [190].

Alternatively, instead of modifying the catalysts composition, the WGS activity of Au/CeO_2-based systems can be influenced by adjusting the reaction conditions (i.e., co-feeding small amount of molecular oxygen in the gas mixture—the so-called "oxygen assisted water gas shift" (OWGS). Indeed, the OWGS is a good approach not only to improve the CO conversion rate but also to mitigate the deactivation effects related to carbonaceous species deposition or ceria over-reduction [190]. Flytzani-Stephanopoulos group's presented a comparison using powder Au and Pt catalysts for OWGS, where small amounts of gaseous oxygen (air) stabilizes nano-structured Au–ceria and Pt–ceria catalysts in H_2-rich gases and start/stop operation [191]. Recently, González-Castaño et al. established some key differences between Au/CeO_2 and Pt/CeO_2 structured catalysts in the OWGS [192]. Apparently, only the gold-based system benefits for an actual "O_2-assisted WGS" reaction; meanwhile, the CO conversion increment observed for the Pt monolith results from the parallel WGS and CO oxidation reaction.

Going back to the stability of Au/CeO_2-based catalysts in the WGS process, their performance under discontinuous operation is especially relevant. For instance, under on-board operation (i.e., hydrogen alimented vehicles), all catalysts involved in the fuel processor (the reforming catalysts, the WGS catalysts, the CO–PROX, or the methanation catalyst) must tolerate the start-up/shut-down cycles of the engine. In fact, that this type of start/stop stability tests are the most demanding proves it can be imagined for a shift catalyst since, during the stop stages, the reactor is cooled down at room temperature with the reactive mixture flowing through the catalytic bed. The latter involves liquid water condensation on the catalysts' porous structure, eventually deactivating the system. Despite the fact that this kind of test seems essential for practical reasons, they are not yet extended enough and few reports can be found in the literature considering these situations [192–195]. In a recent paper, multicomponent Au/CeO_2–CuO/Al_2O_3 catalysts were submitted to a series of start/stop cycles, and its behavior was compared to that presented by an $Au/CuO/Al_2O_3$ catalyst (Figure 11A) [144]. The $Au/CuO/Al_2O_3$ catalyst does not tolerate the start/stop sequences suffering clear deactivation after a series of consecutive cycles. On the contrary, the ceria-containing catalyst (Au/Ce2Cu8/Al) successfully withstands the start/stop operations with no evidence of activity depletion, an encouraging result for realistic application. The presence of ceria seems therefore to be indispensable. The spent sample were analyzed via temperature programmed desorption (TPD), and the CO_2 desorption profiles provide some clues of the Au/CeO_2–CuO system behavior (Figure 11B). The carbonaceous species formed under reaction conditions for the $Au/CuO/Al_2O_3$ catalyst formulation seem to be strongly attached to the catalyst's surface and requires higher temperatures of removal. In contrast, the high oxygen mobility introduced by ceria facilitate carbonate-like species decomposition at lower temperatures [195].

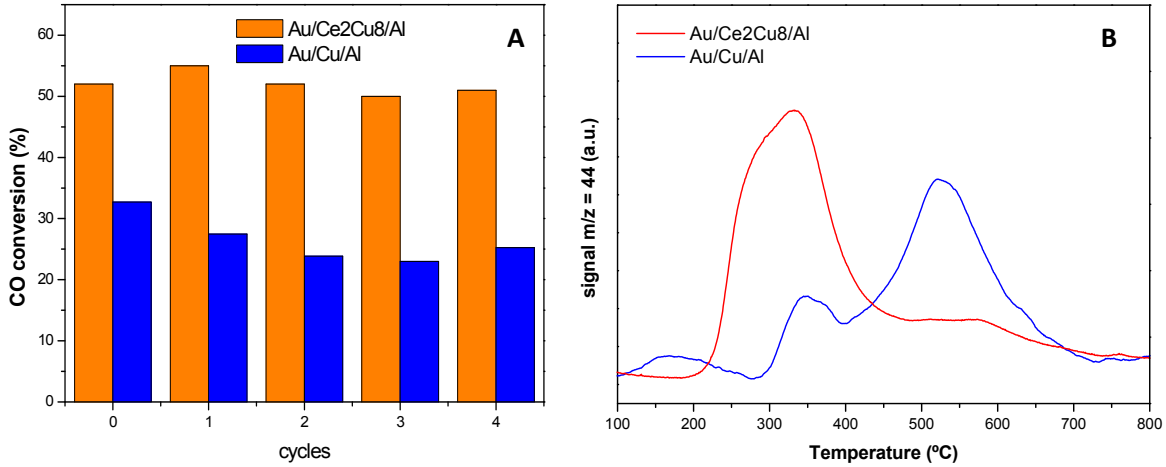

Figure 11. (**A**) Start-up/shut-down stability. Reaction conditions: 50% H_2; 12% CO_2; 30% H_2O; 11% CO after the long-term stability test at 280 °C; (**B**) CO_2-TPD profiles of the spent catalysts after the start-up/shut-down test. Reproduced with permission from [144]. Copyright Elsevier, 2016.

In summary, Au/CeO_2-based systems are among the preferred materials for low- and medium-temperature WGS reaction. Their activity and stability can be considerably upgraded by altering the catalysts' composition (use of ceria dopants, bimetallic formulations, etc.) or by adjusting the reaction conditions (for instance, introducing small amounts of air in the so-called oxygen-assisted WGS). The improved Au/CeO_2 formulations may present enough stability towards start/stop situations, a vital requisite for an intended realistic application.

4.4. Preferential CO Oxidation (CO–PROX)

The production of hydrogen pure enough to feed PEMFC requires further clean-up processes after the WGS unit in order to reduce the CO concentration to compatible levels with the PEMFC (typically 10–50 ppm) [10]. The preferential CO oxidation in rich-H_2 streams (Equation (15)) has been proposed as cheap and efficient alternative for the elimination of the final traces of CO [35–38]. The oxidation reaction is rapid and responds quickly to changes induced in the operating conditions. It is then essential to choose catalysts and operating conditions that minimize the oxidation of hydrogen. In this regard, the control of the reactor temperature is found to be particularly important [10].

$$CO + 1/2O_2 \rightarrow CO_2 \text{ (desired reaction)}; \quad (15)$$

$$H_2 + 1/2O_2 \rightarrow H_2O \text{ (undesired reaction)}. \quad (16)$$

Attending the above-mentioned equations, PROX reaction requires selective catalysts able to abate CO without oxidizing H_2 (Equation (16)). In other words, high CO oxidation activities coupled with low hydrogen ones are essential requirements for the PROX catalysts [38,39]. Various studies have confirmed that the rate of CO oxidation over supported Au catalysts exceeds that of H_2 oxidation [40–43]. Moreover, gold-based catalysts show extraordinarily high activity in the low-temperature range, which is appropriate for fuel cell applications. Earlier studies on Au/CeO_2 catalysts found high activity and good selectivity of those systems in the 70–120 °C temperature range, caused by the active participation of ceria in the oxidation process governed by gold [38,39]. The strong influence of the catalysts' preparation method is a general statement in catalysis by gold, but it seems that for an Au/CeO_2-based catalyst for a PROX reaction, this becomes particularly relevant. For instance, the work of Luengnaruemitchai et al. [196] reflects this issue, showing in their case that the co-precipitation method is by far the best option. The superior activity of the catalyst prepared by co-precipitation seems to be related to structural and morphological reasons. For example,

the ceria crystallite size for the sample prepared by co-precipitation was about 4–5 nm, which is much smaller than those prepared by impregnation and sol–gel methods. The smaller the ceria crystals size, the higher the concentration of oxygen defects and the higher the catalytic activity.

Apart from the preparation method influence, there is still much debate in the literature regarding the stability of gold-based catalysts in the PROX reaction. In an fuel processor, hydrogen would reach the PROX unit together with CO_2 and H_2O; thus, a suitable PROX catalyst must also tolerate high amounts of CO_2 and H_2O present in the reformate stream [196]. In this sense, Au/CeO_2 systems demonstrated sufficient stability with time on stream, in contrast to other gold catalysts, such as Au/Fe_2O_3 [197] and Au/TiO_2 [198], which lost a significant part of their initial activity during the first hours of reaction. A good example of high stability is extracted from the paper of Deng et al. [147], where an Au/CeO_2-based catalyst with low gold content preserves its CO conversion and selectivity during 50 h of continuous operation under the presence of CO_2 and H_2O.

The effect of CO_2 and H_2O in the PROX reaction is a controversial matter. While there is general agreement in the literature that CO_2 negatively affects CO conversion, the effect of water has led to contradictory results. In principle, the presence of both CO_2 and H_2O leads to a competitive adsorption phenomenon, since these co-fed reactants would compete with CO and H_2 upon the arrival to the active sites, thus decreasing overall activity. CO_2 also has an extra effect, which is the formation of stable carbonate-like species on the catalysts' surface, thus acting as site blocking and limiting the accessibility of CO and H_2. Herein, the nature of the support is thought to affect the catalyst behavior in the presence of CO_2; acidic supports seem to be more resistant to deactivation than the basic ones [64]. Based on the latter, most studies have found a decrease in CO oxidation when CO_2 is present [129,147,162,196,199]. In the case of water, some studies have reported a negative effect on the CO abatement ability due to the above-mentioned competitive effect [129]. However, other studies [147,199] found a positive influence of water in the reaction. For example, Liao and co-workers found an improved CO–PROX activity for an $Au–Cu/CeO_2$ catalyst in the presence of steam [199]. They attributed the positive effect of water to several reasons: (i) the promotion of the WGS reaction and, as a result, the CO conversion to CO_2; (ii) the formation of hydroxyl groups via the dissociative adsorption of H_2O on gold, behaving as reactive sites for CO oxidation; and (iii) the promotion of the decomposition of carbonates in the presence of water. The influence of water in the total CO oxidation (not PROX) over Au/CeO_2 samples is also a much-studied issue [23,28,200–202]. In general, a positive effect of water at low temperatures (less than 120 °C) is reported, generally ascribed to the oxidative capabilities of H_2O and to its ability to improve the mobility of oxygen species, favoring the control of the implied redox reactions and assuring the adequate oxidation degree of ceria and gold species. Moreover, the direct involvement of H_2O and OH groups in the activation of O_2 molecules and the transformation of the catalytic intermediates and inhibitors such as the carbonate species have been considered. Some authors also detect an optimal water concentration in the feed-stream, after which the catalytic activity decreases or remains constant.

In a similar way, as for total CO oxidation or WGS, the performance of the Au/CeO_2 catalyst for CO–PROX reaction can be upgraded via ceria doping. As proposed by Avgouropoulos et al., the use of dopant cations with an ionic radius and electronegativity close to those of a cerium cation is considered the most appropriate way to modify cerias' structural and chemical properties [162]. This is related to heterocations' ability to cause structural distortions inside ceria, causing oxide lattice strain and favoring oxygen vacancy formation, which in turn leads to greater oxygen mobility and higher oxidation activity. In particular, Sm and Zn are reported to have a positive impact on the Au/CeO_2 catalyst activity, while La has the opposite effect. Additionally, the promoters also help to achieve greater resistance towards CO_2 poisoning [162]. Zr, Fe, and Zn were proposed by Laguna et al. as very effective ceria promoters, with each dopant causing a different effect on the ceria structural and electronic properties but always positively influencing the catalytic activity [51]. As stated in this work, the formation of the surface oxygen vacancies depends on the nature of the modifier, doping with Zr enhances its formation, while the use of Zn does not influence the vacancies number and Fe makes them

disappear. Nevertheless, a high dispersion of gold nanoparticles is achieved in all cases. During the modification with Zn, the epitaxial interaction between CeO_2 and ZnO creates preferential sites for gold deposition on the interphase between the two oxides. Doping with iron results in a solid solution formation where Fe ions occupy interstitial positions in the CeO_2 structure. These low coordination positions result in electron-rich sites that replace oxygen vacancies for anchoring gold nanoparticles, thus increasing noble metal dispersion and overall activity. More recently, broader dopant screening for the CO–PROX reaction using $Au/CeO_2–MO_x/Al_2O_3$ catalysts with M = La, Ni, Cu, Fe, Cr, and Y has been reported [143]. In this report, Fe and especially Cu were detected as the most promising promoters. Furthermore, the use of alumina as a main support provides several advantages. Dispersing ceria over a high-surface carrier such as alumina results in higher surface-to-bulk ratios, which leads to enhanced OSC of the samples [140]. At the same time, this catalyst configuration only requires a small amount of ceria, which reduces the expense of cerium oxide considerably. The low amount of ceria as support for gold nanoparticles provides an innovative approach to design Au/CeO_2-based catalysts for the PROX reaction.

Although much progress has been made in Au/CeO_2-based catalysts for the CO–PROX reaction, these systems present an inherent drawback which is difficult to overcome. The CO oxidation selectivity of gold-based catalysts is poorer compared to that exhibited by the $CuO–CeO_2$ catalyst, a reference material in the PROX process [203]. Furthermore, the selectivity of Au/CeO_2-based catalysts decreases drastically upon increasing the temperature. This is a consequence of the high activity of gold nanoparticles to burn hydrogen, also confirmed by with kinetics of the processes (normally H_2 oxidation rate superposes that of CO oxidation at medium-high temperatures). As a result, all intended applications of Au/CeO_2 systems are questioned by the selectivity issue. However, the selectivity-to-stability ratio can be modulated by adjusting the reaction parameters, as for example space velocity and CO-to-O_2 ratio (lambda parameter). As recently reported elsewhere [129], for low lambda values, lower CO conversion is obtained, although with high selectivity due to the preferential reaction between the available oxygen and CO, especially at low temperatures. For high lambda values, greater activity for both CO and hydrogen oxidation was observed, thus decreasing the overall selectivity. The contact time is also a point to consider for improving the conversion-to-selectivity ratio. In this case, both conversion and selectivity follow the same trend: the higher the space velocity, the lower the conversion and selectivity. In other words, the conversion-to-selectivity balance can be improved by increasing the contact time between the reactive molecules and the catalyst [129]. Tuning these parameters, a good performance can be achieved by Au/CeO_2-based catalysts. For example, a Cu-doped $Au/CeO_2/Al_2O_3$ catalyst has exhibited high activity (95% of CO conversion) and good selectivity (55% towards CO_2) in a suitable temperature range (around 110 °C) [143]. On the other hand, the selectivity in PROX reactions is greatly influenced by the supports. In this sense, supports with suppressed activity for hydrogen oxidation are a logical alternative [161]. Finally, to improve the selectivity of the process, it is strongly recommended that hydrogen and carbon monoxide oxidation is split and that each reaction is studied separately [161]. This approach provides an in-depth understanding of the selectivity trends bringing fundamental knowledge to tailor the activity-to-selectivity balance towards more efficient CO–PROX catalysts.

5. Conclusions

All the bibliographic works described and discussed in this comprehensive review highlight the importance of Au/CeO_2-based catalysts for potential application in various oxidation reactions. The number of scientific papers considering such materials is continuously growing, and it is foreseen that this trend will remain in the next future. The extremely high activity of gold nanoparticles in almost all, selective, or total oxidation reactions is indisputable. Although the gold metal appears to be very versatile as a catalyst, its activity obeys certain rules, the presence of nanoparticles (2–3 nm) stabilized on "active support" being the most important. One of those "active" supports is cerium oxide due to its unique structure and redox behaviour. The most important feature of this oxide is

the possibility for easy modification of its oxygen storage capacity and resulting ability to activate oxygen species.

On first sight, the combination of both phases should result only in benefit, and it is the case in a perfect situation. However, every reaction is a "brave new world". The gold deposition method and support modification and formulation should be perfectly adapted to the characteristics demanded by the reaction, which is not an easy task. The CO total oxidation needs a maximal oxygen vacancy population in order to maintain an oxygen activation rate high enough to oxidize every single CO molecule, whereas for WGS and PROX an optimal number of defects is needed in order to suppress the causes of deactivation or decrease in selectivity. Not only is the catalytic system important, but the process parameters should also be adapted to the application requirements. It is possible in some cases to fulfill the requisites without applying the most performant system. An important approach for this is, for example, the use of CeO_2–Al_2O_3 system instead of bare CeO_2. The former presents higher a ceria surface-to-bulk ratio, thus optimizing ceria redox properties and presenting a cheaper and easier way to modify material.

Although in the last decade, Au/CeO_2-based catalysts are within the most popular gold-based systems for CO oxidation reactions, the complexity of the interaction between gold and ceria makes the control and elucidation of the specific active site that controls the reaction mechanism of every considered oxidation reaction a difficult task and still seeks general agreement. Moreover, a variety of new oxidation reactions in liquid phase will open new horizons for the Au/CeO_2 system. There is still much work to be done, but it could be helpful to remember that the reaction provides the requisites, and the system provides the possibilities.

Acknowledgments: The authors are grateful to the support from the Spanish Ministerio de Economía y Competitividad (MINECO) (ENE2015-66975-C3-2-R and ENE2013-47880-C3-2-R) and from Junta de Andalucía (TEP-8196) co-financed by FEDER funds from the European Union. The financial support from Junta de Andalucía of the "Surface Chemistry and Catalysis" research group (TEP106) is specifically acknowledged.

Author Contributions: In this review, all the authors have contributed in a solidary way to the revision of the considered literature data. Tomás Ramírez Reina, Oscar Hernando Laguna and Svetlana Ivanova have written different parts of the manuscript, selecting and modifying the figures presented. José Antonio Odriozola and Miguel Angel Centeno have revised, and gave uniformity to the final version of paper.

Conflicts of Interest: The authors declare no conflict of interest.

References

1. Raub, J.A.; Mathieu-Nolf, M.; Hampson, N.B.; Thom, S.R. Carbon monoxide poisoning—A public health perspective. *Toxicology* **2000**, *145*, 1–14. [CrossRef]
2. Royer, S.; Duprez, D. Catalytic oxidation of carbon monoxide over transition metal oxides. *ChemCatChem* **2011**, *3*, 24–65. [CrossRef]
3. Haruta, M.; Kobayashi, T.; Sano, H.; Yamada, N. Novel gold catalysts for the oxidation of carbon-monoxide at a temperature far below 0. DEG. C. *Chem. Lett.* **1987**, *16*, 405–408. [CrossRef]
4. Bond, G.C.; Thompson, D.T. Gold-catalysed oxidation of carbon monoxide. *Gold Bull.* **2000**, *33*, 41–51. [CrossRef]
5. Haruta, M. Catalysis of gold nanoparticles deposited on metal oxides. *Cattech* **2002**, *6*, 102–115. [CrossRef]
6. Chen, M.S.; Goodman, D.W. Structure-activity relationships in supported Au catalysts. *Catal. Today* **2006**, *111*, 22–33. [CrossRef]
7. Corma, A.; García, H. Supported gold nanoparticles as oxidation catalysts. In *Nanoparticles and Catalysis*; Astruc, D., Ed.; Willey-VCH Verlag GmbH & Co. KGaA: Weinheim, Germany, 2008; pp. 389–429.
8. Corti, C.W.; Holliday, R.J.; Thompson, D.T. Progress towards the commercial application of gold catalysts. *Top. Catal.* **2007**, *44*, 331–343. [CrossRef]
9. Cortie, M.; Laguna, A.; Thompson, D. Gold 2006 highlights of 4th international conference on the science, technology and industrial applications of gold. *Gold Bull.* **2006**, *39*, 226–235. [CrossRef]
10. Trimm, D.L. Minimisation of carbon monoxide in a hydrogen stream for fuel cell application. *Appl. Catal. A* **2005**, *296*, 1–11. [CrossRef]

11. Laguna, O.H.; Pérez, A.; Centeno, M.A.; Odriozola, J.A. Synergy between gold and oxygen vacancies in gold supported on Zr-doped ceria catalysts for the CO oxidation. *Appl. Catal. B* **2015**, *177*, 385–395. [CrossRef]
12. Romero-Sarria, F.; Plata, J.J.; Laguna, O.H.; Márquez, A.M.; Centeno, M.A.; Sanz, J.F.; Odriozola, J.A. Surface oxygen vacancies in gold based catalysts for CO oxidation. *RSC Adv.* **2014**, *4*, 13145–13152. [CrossRef]
13. Milt, V.G.; Ivanova, S.; Sanz, O.; Dominguez, M.I.; Corrales, A.; Odriozola, J.A.; Centeno, M.A. Au/TiO_2 supported on ferritic stainless steel monoliths as CO oxidation catalysts. *Appl. Surf. Sci.* **2013**, *270*, 169–177. [CrossRef]
14. Reina, T.R.; Moreno, A.A.; Ivanova, S.; Odriozola, J.A.; Centeno, M.A. Influence of vanadium or cobalt oxides on the CO oxidation behavior of Au/MOx/CeO_2–Al_2O_3 systems. *ChemCatChem* **2012**, *4*, 512–520. [CrossRef]
15. Reina, T.R.; Ivanova, S.; Domínguez, M.I.; Centeno, M.A.; Odriozola, J.A. Sub-ambient CO oxidation over Au/MOx/CeO_2–Al_2O_3 (M = Zn or Fe). *Appl. Catal. A* **2012**, *420*, 58–66. [CrossRef]
16. Romero-Sarria, F.; Dominguez, M.I.; Centeno, M.A.; Odriozola, J.A. CO oxidation at low temperature on Au/$CePO_4$: Mechanistic aspects. *Appl. Catal. B* **2011**, *107*, 268–273. [CrossRef]
17. Laguna, O.H.; Centeno, M.A.; Romero-Sarria, F.; Odriozola, J.A. Oxidation of CO over gold supported on Zn-modified ceria catalysts. *Catal. Today* **2011**, *172*, 118–123. [CrossRef]
18. Plata, J.J.; Marquez, A.M.; Sanz, J.F.; Avellaneda, R.S.; Romero-Sarria, F.; Dominguez, M.I.; Centeno, M.A.; Odriozola, J.A. Gold nanoparticles on yttrium modified titania: Support properties and catalytic activity. *Top. Catal.* **2011**, *54*, 219–228. [CrossRef]
19. Laguna, O.H.; Centeno, M.A.; Arzamendi, G.; Gandía, L.M.; Romero-Sarria, F.; Odriozola, J.A. Iron-modified ceria and Au/ceria catalysts for total and preferential oxidation of CO (TOX and PROX). *Catal. Today* **2010**, *157*, 155–159. [CrossRef]
20. Hernández, W.Y.; Romero-Sarria, F.; Centeno, M.A.; Odriozola, J.A. In Situ Characterization of the dynamic gold-support interaction over ceria modified Eu^{3+}. Influence of the oxygen vacancies on the CO oxidation reaction. *J. Phys. Chem. C* **2010**, *114*, 10857–10865. [CrossRef]
21. Domínguez, M.I.; Romero-Sarria, F.; Centeno, M.A.; Odriozola, J.A. Gold/hydroxyapatite catalysts: Synthesis, characterization and catalytic activity to CO oxidation. *Appl. Catal. B* **2009**, *87*, 245–251. [CrossRef]
22. Penkova, A.; Chakarova, K.; Laguna, O.H.; Hadjiivanov, K.; Saria, F.R.; Centeno, M.A.; Odriozola, J.A. Redox chemistry of gold in a Au/FeOx/CeO_2 CO oxidation catalyst. *Catal. Commun.* **2009**, *10*, 1196–1202. [CrossRef]
23. Romero-Sarria, F.; Penkova, A.; Martinez, T.L.M.; Centeno, M.A.; Hadjiivanov, K.; Odriozola, J.A. Role of water in the CO oxidation reaction on Au/CeO_2: Modification of the surface properties. *Appl. Catal. B* **2008**, *84*, 119–124. [CrossRef]
24. Centeno, M.A.; Hidalgo, M.C.; Dominguez, M.I.; Navio, J.A.; Odriozola, J.A. Titania-supported gold catalysts: Comparison between the photochemical phenol oxidation and gaseous CO oxidation performances. *Catal. Lett.* **2008**, *123*, 198–206. [CrossRef]
25. Romero-Sarria, F.; Martinez, L.M.; Centeno, M.A.; Odriozola, J.A. Surface dynamics of Au/CeO_2 catalysts during CO oxidation. *J. Phys. Chem. C* **2007**, *111*, 14469–14475. [CrossRef]
26. Centeno, M.A.; Hadjiivanov, K.; Venkov, T.; Klimev, H.; Odriozola, J.A. Comparative study of Au/Al_2O_3 and Au/CeO_2–Al_2O_3 catalysts. *J. Mol. Catal. A* **2006**, *252*, 142–149. [CrossRef]
27. Centeno, M.A.; Carrizosa, I.; Odriozola, J.A. Deposition-precipitation method to obtain supported gold catalysts: Dependence of the acid-base properties of the support exemplified in the system TiO_2–TiOxNy–TiN. *Appl. Catal. A* **2003**, *246*, 365–372. [CrossRef]
28. Centeno, M.A.; Portales, C.; Carrizosa, I.; Odriozola, J.A. Gold supported CeO_2/Al_2O_3 catalysts for CO oxidation: Influence of the ceria phase. *Catal. Lett.* **2005**, *102*, 289–297. [CrossRef]
29. Hashmi, A.S.K.; Hutchings, G.J. Gold catalysis. *Angew. Chem. Int. Ed.* **2006**, *45*, 7896–7936. [CrossRef] [PubMed]
30. Ivanova, S.; Laguna, O.H.; Centeno, M.A.; Eleta, A.; Montes, M.; Odriozola, J.A. Microprocess technology for hydrogen purification. In *Renewable Hydrogen Technologies*; Diéguez, P.M., Gandía, L.M., Arzamendi, G., Eds.; Elsevier: Amsterdam, The Netherlands, 2013; pp. 225–243.
31. Arzamendi, G.; Diéguez, P.M.; Montes, M.; Centeno, M.A.; Odriozola, J.A.; Gandía, L.M. Integration of methanol steam reforming and combustion in a microchannel reactor for H_2 production: A CFD simulation study. *Catal. Today* **2009**, *143*, 25–31. [CrossRef]
32. Burch, R. Gold catalysts for pure hydrogen production in the water-gas shift reaction: Activity, structure and reaction mechanism. *Phys. Chem. Chem. Phys.* **2006**, *8*, 5483–5500. [CrossRef] [PubMed]

33. Ratnasamy, C.; Wagner, J.P. Water gas shift catalysis. *Catal. Rev. Sci. Eng.* **2009**, *51*, 325–440. [CrossRef]
34. Fu, Q.; Saltsburg, H.; Flytzani-Stephanopoulos, M. Active nonmetallic Au and Pt species on ceria-based water-gas shift catalysts. *Science* **2003**, *301*, 935–938. [CrossRef] [PubMed]
35. Fujita, S.-I.; Takezawa, N. Difference in the selectivity of CO and CO_2 methanation reactions. *Chem. Eng. J.* **1997**, *68*, 63–68. [CrossRef]
36. Golunski, S. HotSpot™ fuel processor. *Platin. Met. Rev.* **1998**, *42*, 2–7.
37. Avgouropoulos, G.; Ioannides, T. Selective CO oxidation over CuO–CeO_2 catalysts prepared via the urea–nitrate combustion method. *Appl. Catal. A* **2003**, *244*, 155–167. [CrossRef]
38. Choudhary, T.V.; Goodman, D.W. CO-free fuel processing for fuel cell applications. *Catal. Today* **2002**, *77*, 65–78. [CrossRef]
39. Shodiya, T.; Schmidt, O.; Peng, W.; Hotz, N. Novel nano-scale Au/α-Fe_2O_3 catalyst for the preferential oxidation of CO in biofuel reformate gas. *J. Catal.* **2013**, *300*, 63–69. [CrossRef]
40. Grisel, R.; Weststrate, K.J.; Gluhoi, A.; Nieuwenhuys, B.E. Catalysis by gold nanoparticles. *Gold Bull.* **2002**, *35*, 39–45. [CrossRef]
41. Grisel, R.J.H.; Nieuwenhuys, B.E. Selective oxidation of CO, over supported Au catalysts. *J. Catal.* **2001**, *199*, 48–59. [CrossRef]
42. Haruta, M.; Tsubota, S.; Kobayashi, T.; Kageyama, H.; Genet, M.J.; Delmon, B. Low-temperature oxidation of CO over gold supported on TiO_2, α-Fe_2O_3, and Co_3O_4. *J. Catal.* **1993**, *144*, 175–192. [CrossRef]
43. Sanchez, R.M.T.; Ueda, A.; Tanaka, K.; Haruta, M. Selective oxidation of CO in hydrogen over gold supported on manganese oxides. *J. Catal.* **1997**, *168*, 125–127. [CrossRef]
44. Hernández, W.Y.; Centeno, M.A.; Romero-Sarria, F.; Ivanova, S.; Montes, M.; Odriozola, J.A. Modified cryptomelane-type manganese dioxide nanomaterials for preferential oxidation of CO in the presence of hydrogen. *Catal. Today* **2010**, *157*, 160–165. [CrossRef]
45. Andreeva, D.; Idakiev, V.; Tabakova, T.; Andreev, A.; Giovanoli, R. Low-temperature water-gas shift reaction on Auα-Fe_2O_3 catalyst. *Appl. Catal. A* **1996**, *134*, 275–283. [CrossRef]
46. Wang, H.; Zhu, H.; Qin, Z.; Liang, F.; Wang, G.; Wang, J. Deactivation of a Au/CeO_2–Co_3O_4 catalyst during CO preferential oxidation in H_2-rich stream. *J. Catal.* **2009**, *264*, 154–162. [CrossRef]
47. Trovarelli, A. Catalytic properties of ceria and CeO_2-containing materials. *Catal. Rev. Sci. Eng.* **1996**, *38*, 439–520. [CrossRef]
48. Trovarelli, A. Structural properties and nonstoichiometric behavior of CeO_2. In *Catalysis by Ceria and Related Materials*; Trovarelli, A., Ed.; Imperial College Press: London, UK, 2002; pp. 15–50.
49. Aneggi, E.; Boaro, M.; Leitenburg, C.D.; Dolcetti, G.; Trovarelli, A. Insights into the dynamics of oxygen storage/release phenomena in model ceria–zirconia catalysts as inferred from transient studies using H_2, CO and soot as reductants. *Catal. Today* **2006**, *112*, 94–98. [CrossRef]
50. Fonseca, A.A.; Fisher, J.M.; Ozkaya, D.; Shannon, M.D.; Thompsett, D. Ceria-zirconia supported Au as highly active low temperature water-gas shift catalysts. *Top. Catal.* **2007**, *44*, 223–235. [CrossRef]
51. Laguna, O.H.; Sarria, F.R.; Centeno, M.A.; Odriozola, J.A. Gold supported on metal-doped ceria catalysts (M = Zr, Zn and Fe) for the preferential oxidation of CO (PROX). *J. Catal.* **2010**, *276*, 360–370. [CrossRef]
52. Bao, H.Z.; Chen, X.; Fang, J.; Jiang, Z.Q.; Huang, W.X. Structure-activity relation of Fe_2O_3–CeO_2 composite catalysts in CO oxidation. *Catal. Lett.* **2008**, *125*, 160–167. [CrossRef]
53. Laguna, O.H.; Centeno, M.A.; Boutonnet, M.; Odriozola, J.A. Fe-doped ceria solids synthesized by the microemulsion method for CO oxidation reactions. *Appl. Catal. B* **2011**, *106*, 621–629. [CrossRef]
54. Abu-Zied, B.M.; Soliman, S.A. Thermal decomposition of praseodymium acetate as a precursor of praseodymium oxide catalyst. *Thermochim. Acta* **2008**, *470*, 91–97. [CrossRef]
55. Bueno-López, A.; Krishna, K.; Makkee, M.; Moulijn, J.A. Enhanced soot oxidation by lattice oxygen via La^{3+}-doped CeO_2. *J. Catal.* **2005**, *230*, 237–248. [CrossRef]
56. Hernández, W.Y.; Laguna, O.H.; Centeno, M.A.; Odriozola, J.A. Structural and catalytic properties of lanthanide (La, Eu, Gd) doped ceria. *J. Solid State Chem.* **2011**, *184*, 3014–3020. [CrossRef]
57. Hernández, W.Y.; Centeno, M.A.; Romero-Sarria, F.; Odriozola, J.A. Synthesis and Characterization of $Ce_{1-x}Eu_xO_{2-x/2}$ Mixed Oxides and Their Catalytic Activities for CO Oxidation. *J. Phys. Chem. C* **2009**, *113*, 5629–5635. [CrossRef]
58. Wang, F.; Lu, G. High performance rare earth oxides LnO_x (Ln = La, Ce, Nd, Sm and Dy)-modified Pt/SiO_2 catalysts for CO oxidation in the presence of H_2. *J. Power Sources* **2008**, *181*, 120–126. [CrossRef]

59. Gellings, P.J.; Bouwmeester, H.J.M. Ion and mixed conducting oxides as catalysts. *Catal. Today* **1992**, *12*, 1–101. [CrossRef]
60. Bond, G.C.; Louis, C.; Thompson, D.T. Catalysis by gold. In *Catalytic Science Series*; Hutchings, G.J., Ed.; Imperial College Press: London, UK, 2006; pp. 180–182.
61. Ma, Z.; Dai, S. *Heterogeneous Gold Catalysts and Catalysis*; The Royal Society of Chemistry: London, UK, 2014.
62. Corma, A.; Garcia, H. Supported gold nanoparticles as catalysts for organic reactions. *Chem. Soc. Rev.* **2008**, *37*, 2096–2126. [CrossRef] [PubMed]
63. Corma, A. Attempts to fill the gap between enzymatic, homogeneous, and heterogeneous catalysis. *Catal. Rev. Sci. Eng.* **2004**, *46*, 369–417. [CrossRef]
64. Bond, G.C.; Thompson, D.T. Catalysis by gold. *Catal. Rev. Sci. Eng.* **1999**, *41*, 319–388. [CrossRef]
65. Barakat, T.; Rooke, J.C.; Genty, E.; Cousin, R.; Siffert, S.; Su, B.-L. Gold catalysts in environmental remediation and water-gas shift technologies. *Energy Environ. Sci.* **2013**, *6*, 371–391. [CrossRef]
66. Haruta, M. Gold as a novel catalyst in the 21st century: Preparation, working mechanism and applications. *Gold Bull.* **2004**, *37*, 27–36. [CrossRef]
67. Whyman, R. Gold nanoparticles a renaissance in gold chemistry. *Gold Bull.* **1996**, *29*, 11–15. [CrossRef]
68. Tao, F.; Ma, Z. Water-gas shift on gold catalysts: Catalyst systems and fundamental studies. *Phys. Chem. Chem. Phys.* **2013**, *15*, 15260–15270. [CrossRef] [PubMed]
69. Hutchings, G.J. Catalysis: A golden future. *Gold Bull.* **1996**, *29*, 123–130. [CrossRef]
70. Haruta, M. Size- and support-dependency in the catalysis of gold. *Catal. Today* **1997**, *36*, 153–166. [CrossRef]
71. Haruta, M.; Date, M. Advances in the catalysis of Au nanoparticles. *Appl. Catal. A* **2001**, *222*, 427–437. [CrossRef]
72. Hutchings, G.J. Gold catalysis in chemical processing. *Catal. Today* **2002**, *72*, 11–17. [CrossRef]
73. Thompson, D.T. Perspective on industrial and scientific aspects of gold catalysis. *Appl. Catal. A* **2003**, *243*, 201–205. [CrossRef]
74. Cameron, D.; Holliday, R.; Thompson, D. Gold's future role in fuel cell systems. *J. Power Sources* **2003**, *118*, 298–303. [CrossRef]
75. Corti, C.W.; Holliday, R.J.; Thompson, D.T. Commercial aspects of gold catalysis. *Appl. Catal. A* **2005**, *291*, 253–261. [CrossRef]
76. Hutchings, G.J. Catalysis by gold. *Catal. Today* **2005**, *100*, 55–61. [CrossRef]
77. Bond, G.C.; Thompson, D.T. Status of catalysis by gold following an AURICAT Workshop. *Appl. Catal. A* **2006**, *302*, 1–4. [CrossRef]
78. Scirè, S.; Liotta, L.F. Supported gold catalysts for the total oxidation of volatile organic compounds. *Appl. Catal. B* **2012**, *125*, 222–246. [CrossRef]
79. Chen, M.; Goodman, D.W. Catalytically active gold: From nanoparticles to ultrathin films. *Acc. Chem. Res.* **2006**, *39*, 739–746. [CrossRef] [PubMed]
80. Gorin, D.J.; Toste, F.D. Relativistic effects in homogeneous gold catalysis. *Nature* **2007**, *446*, 395–403. [CrossRef] [PubMed]
81. Hamilton, G.L.; Kang, E.J.; Mba, M.; Toste, F.D. A powerful chiral counterion strategy for asymmetric transition metal catalysis. *Science* **2007**, *317*, 496–499. [CrossRef] [PubMed]
82. Haruta, A. When gold is not noble: Catalysis by nanoparticles. *Chem. Rec.* **2003**, *3*, 75–87. [CrossRef] [PubMed]
83. Hashmi, A.S.K. Homogeneous catalysis by gold. *Gold Bull.* **2004**, *37*, 51–65.
84. Hashmi, A.S.K. The catalysis gold rush: New claims. *Angew. Chem. Int. Ed.* **2005**, *44*, 6990–6993. [CrossRef] [PubMed]
85. Hutchings, G.J.; Carrettin, S.; Landon, P.; Edwards, J.K.; Enache, D.; Knight, D.W.; Xu, Y.-J.; Carley, A.F. New approaches to designing selective oxidation catalysts: Au/C a versatile catalyst. *Top. Catal.* **2006**, *38*, 223–230. [CrossRef]
86. Kung, M.C.; Davis, R.J.; Kung, H.H. Understanding Au-catalyzed low-temperature CO oxidation. *J. Phys. Chem. C* **2007**, *111*, 11767–11775. [CrossRef]
87. Liotta, L.F. New frontiers in gold catalyzed reactions. *Catalysts* **2012**, *2*, 299–302. [CrossRef]
88. Mihaylov, M.; Knoezinger, H.; Hadjiivanov, K.; Gates, B.C. Characterization of the oxidation states of supported gold species by IR spectroscopy of adsorbed CO. *Chem. Ing. Tech.* **2007**, *79*, 795–806. [CrossRef]

89. Pattrick, G.; van der Lingen, E.; Corti, C.W.; Holliday, R.J.; Thompson, D.T. The potential for use of gold in automotive pollution control technologies: A short review. *Top. Catal.* **2004**, *1*, 273–279. [CrossRef]
90. Thompson, D. New advances in gold catalysis part I. *Gold Bull.* **1998**, *31*, 111–118. [CrossRef]
91. Thompson, D.T. Catalysis by gold/platinum group metals. Mixed metal systems displaying increased activity. *Platin. Met. Rev.* **2004**, *48*, 169–172. [CrossRef]
92. Thompson, D.T. An overview of gold-catalysed oxidation processes. *Top. Catal.* **2006**, *38*, 231–240. [CrossRef]
93. Thompson, D.T. Using gold nanoparticles for catalysis. *Nano Today* **2007**, *2*, 40–43. [CrossRef]
94. Fu, Q.; Kudriavtseva, S.; Saltsburg, H.; Flytzani-Stephanopoulos, M. Gold–ceria catalysts for low-temperature water-gas shift reaction. *Chem. Eng. J.* **2003**, *93*, 41–53. [CrossRef]
95. Tabakova, T.; Boccuzzi, F.; Manzoli, M.; Sobczak, J.W.; Idakiev, V.; Andreeva, D. Effect of synthesis procedure on the low-temperature WGS activity of Au/ceria catalysts. *Appl. Catal. B* **2004**, *49*, 73–81. [CrossRef]
96. Zanella, R.; Giorgio, S.; Henry, C.R.; Louis, C. Alternative methods for the preparation of gold nanoparticles supported on TiO_2. *J. Phys. Chem. B* **2002**, *106*, 7634–7642. [CrossRef]
97. Ivanova, S.; Pitchon, V.; Petit, C. Application of the direct exchange method in the preparation of gold catalysts supported on different oxide materials. *J. Mol. Catal. A* **2006**, *256*, 278–283. [CrossRef]
98. Ivanova, S.; Petit, C.; Pitchon, V. A new preparation method for the formation of gold nanoparticles on an oxide support. *Appl. Catal. A* **2004**, *267*, 191–201. [CrossRef]
99. Ivanova, S.; Pitchon, V.; Zimmermann, Y.; Petit, C. Preparation of alumina supported gold catalysts: Influence of washing procedures, mechanism of particles size growth. *Appl. Catal. A* **2006**, *298*, 57–64. [CrossRef]
100. Bredig, G.; Reinders, W. Anorganic enzymes. III. The gold catalysis of hydrogen peroxide. *Z. Phys. Chem. Stochiometrie Verwandtschaftslehre* **1901**, *37*, 323–341.
101. Prati, L.; Rossi, M. Gold on carbon as a new catalyst for selective liquid phase oxidation of diols. *J. Catal.* **1998**, *176*, 552–560. [CrossRef]
102. Prati, L.; Martra, G. New gold catalysts for liquid phase oxidation. *Gold Bull.* **1999**, *32*, 96–101. [CrossRef]
103. Prati, L.; Villa, A.; Lupini, A.R.; Veith, G.M. Gold on carbon: One billion catalysts under a single label. *Phys. Chem. Chem. Phys.* **2012**, *14*, 2969–2978. [CrossRef] [PubMed]
104. Lakshmanan, P.; Upare, P.P.; Le, N.-T.; Hwang, Y.K.; Hwang, D.W.; Lee, U.H.; Kim, H.R.; Chang, J.-S. Facile synthesis of CeO_2-supported gold nanoparticle catalysts for selective oxidation of glycerol into lactic acid. *Appl. Catal. A* **2013**, *468*, 260–268. [CrossRef]
105. Hutchings, G.J. Catalyst synthesis using supercritical carbon dioxide: A green route to high activity materials. *Top. Catal.* **2009**, *52*, 982–987. [CrossRef]
106. Miedziak, P.J.; Tang, Z.; Davies, T.E.; Enache, D.I.; Bartley, J.K.; Carley, A.F.; Herzing, A.A.; Kiely, C.J.; Taylor, S.H.; Hutchings, G.J. Ceria prepared using supercritical antisolvent precipitation: A green support for gold-palladium nanoparticles for the selective catalytic oxidation of alcohols. *J. Mater. Chem.* **2009**, *19*, 8619–8627. [CrossRef]
107. Qu, Y.H.; Liu, F.; Wei, Y.; Gu, C.L.; Zhang, L.H.; Liu, Y. Forming ceria shell on Au-core by LSPR photothermal induced interface reaction. *Appl. Surf. Sci.* **2015**, *343*, 207–211. [CrossRef]
108. Mitsudome, T.; Yamamoto, M.; Maeno, Z.; Mizugaki, T.; Jitsukawa, K.; Kaneda, K. One-step synthesis of core-gold/shell-ceria nanomaterial and its catalysis for highly selective semihydrogenation of alkynes. *J. Am. Chem. Soc.* **2015**, *137*, 13452–13455. [CrossRef] [PubMed]
109. Bera, P.; Hegde, M.S. Characterization and catalytic properties of combustion synthesized Au/CeO_2 catalyst. *Catal. Lett.* **2002**, *79*, 75–81. [CrossRef]
110. Yang, Y.; Saoud, K.M.; Abdelsayed, V.; Glaspell, G.; Deevi, S.; El-Shall, M.S. Vapor phase synthesis of supported Pd, Au, and unsupported bimetallic nanoparticle catalysts for CO oxidation. *Catal. Commun.* **2006**, *7*, 281–284. [CrossRef]
111. Potemkin, D.I.; Semitut, E.Y.; Shubin, Y.V.; Plyusnin, P.E.; Snytnikov, P.V.; Makotchenko, E.V.; Osadchii, D.Y.; Svintsitskiy, D.A.; Venyaminov, S.A.; Korenev, S.V.; et al. Silica, alumina and ceria supported Au–Cu nanoparticles prepared via the decomposition of $[Au(en)_2]_2[Cu(C_2O_4)_2]_3 \cdot 8H_2O$ single-source precursor: Synthesis, characterization and catalytic performance in CO PROX. *Catal. Today* **2014**, *235*, 103–111. [CrossRef]
112. Li, W.; Ge, Q. Oxide-supported $Au_n(SR)_m$ nanoclusters for CO oxidation. *Chin. J. Catal.* **2015**, *36*, 135–138. [CrossRef]
113. Reina, T.R.; Ivanova, S.; Centeno, M.A.; Odriozola, J.A. Low-temperature CO oxidation on multicomponent gold based catalysts. *Front. Chem.* **2013**. [CrossRef]

114. Escamilla-Perea, L.; Nava, R.; Pawelec, B.; Rosmaninho, M.G.; Peza-Ledesma, C.L.; Fierro, J.L.G. SBA-15-supported gold nanoparticles decorated by CeO_2: Structural characteristics and CO oxidation activity. *Appl. Catal. A* **2010**, *381*, 42–53. [CrossRef]
115. Hernandez, J.A.; Gómez, S.; Pawelec, B.; Zepeda, T.A. CO oxidation on Au nanoparticles supported on wormhole HMS material: Effect of support modification with CeO_2. *Appl. Catal. B* **2009**, *89*, 128–136. [CrossRef]
116. Carabineiro, S.A.C.; Bastos, S.S.T.; Órfão, J.J.M.; Pereira, M.F.R.; Delgado, J.J.; Figueiredo, J.L. Exotemplated ceria catalysts with gold for CO oxidation. *Appl. Catal. A* **2010**, *381*, 150–160. [CrossRef]
117. Carabineiro, S.A.C.; Silva, A.M.T.; Dražić, G.; Tavares, P.B.; Figueiredo, J.L. Gold nanoparticles on ceria supports for the oxidation of carbon monoxide. *Catal. Today* **2010**, *154*, 21–30. [CrossRef]
118. Carabineiro, S.A.C.; Silva, A.M.T.; Dražić, G.; Tavares, P.B.; Figueiredo, J.L. Effect of chloride on the sinterization of Au/CeO_2 catalysts. *Catal. Today* **2010**, *154*, 293–302. [CrossRef]
119. Liu, Y.; Liu, B.; Wang, Q.; Li, C.; Hu, W.; Liu, Y.; Jing, P.; Zhao, W.; Zhang, J. Three-dimensionally ordered macroporous Au/CeO_2–Co_3O_4 catalysts with mesoporous walls for enhanced CO preferential oxidation in H_2-rich gases. *J. Catal.* **2012**, *296*, 65–76. [CrossRef]
120. Ta, N.; Liu, J.; Shen, W. Tuning the shape of ceria nanomaterials for catalytic applications. *Chin. J. Catal.* **2013**, *34*, 838–850. [CrossRef]
121. Yuan, Q.; Duan, H.-H.; Li, L.-L.; Sun, L.-D.; Zhang, Y.-W.; Yan, C.-H. Controlled synthesis and assembly of ceria-based nanomaterials. *J. Colloid Interface Sci.* **2009**, *335*, 151–167. [CrossRef] [PubMed]
122. Huang, X.-S.; Sun, H.; Wang, L.-C.; Liu, Y.-M.; Fan, K.-N.; Cao, Y. Morphology effects of nanoscale ceria on the activity of Au/CeO_2 catalysts for low-temperature CO oxidation. *Appl. Catal. B* **2009**, *90*, 224–232. [CrossRef]
123. Jia, K.; Zhang, H.; Li, W. Effect of the morphology of the ceria support on the activity of Au/CeO_2 catalysts for CO oxidation. *Chin. J. Catal.* **2008**, *29*, 1089–1092. [CrossRef]
124. Liu, W.; Deng, T.; Feng, L.; Xie, A.; Zhang, J.; Wang, S.; Liu, X.; Yang, Y.; Guo, J. Designed synthesis and formation mechanism of CeO_2 hollow nanospheres and their facile functionalization with Au nanoparticles. *Crystengcomm* **2015**, *17*, 4850–4858. [CrossRef]
125. Zhu, F.; Chen, G.; Sun, S.; Sun, X. In situ growth of $Au@CeO_2$ core-shell nanoparticles and CeO_2 nanotubes from $Ce(OH)CO_3$ nanorods. *J. Mater. Chem. A* **2013**, *1*, 288–294. [CrossRef]
126. Zhang, Y.; Xu, Y.; Zhou, Y.; Xiang, S.; Sheng, X.; Wang, Q.; Zhang, C. Hierarchical structures based on gold nanoparticles embedded into hollow ceria spheres and mesoporous silica layers with high catalytic activity and stability. *New J. Chem.* **2015**, *39*, 9372–9379. [CrossRef]
127. Laguna, O.H.; Dominguez, M.I.; Romero-Sarria, F.; Odriozola, J.A.; Centeno, M.A. Role of oxygen vacancies in gold oxidation catalysis. In *Heterogeneous Gold Catalysts and Catalysis*; Ma, Z., Dai, S., Eds.; The Royal Society of Chemistry: London, UK, 2014; pp. 489–511.
128. Guzman, J.; Carrettin, S.; Corma, A. Spectroscopic evidence for the supply of reactive oxygen during CO oxidation catalyzed by gold supported on nanocrystalline CeO_2. *J. Am. Chem. Soc.* **2005**, *127*, 3286–3287. [CrossRef] [PubMed]
129. Reina, T.R.; Papadopoulou, E.; Palma, S.; Ivanova, S.; Centeno, M.A.; Ioannides, T.; Odriozola, J.A. Could an efficient WGS catalyst be useful in the CO–PrOx reaction? *Appl. Catal. B* **2014**, *150–151*, 554–563. [CrossRef]
130. Reina, T.R.; Ivanova, S.; Idakiev, V.; Tabakova, T.; Centeno, M.A.; Deng, Q.-F.; Yuan, Z.-Y.; Odriozola, J.A. Nanogold mesoporous iron promoted ceria catalysts for total and preferential CO oxidation reactions. *J. Mol. Catal. A* **2016**, *414*, 62–71. [CrossRef]
131. Shapovalov, V.; Metiu, H. Catalysis by doped oxides: CO oxidation by $Au_xCe_{1-x}O_2$. *J. Catal.* **2007**, *245*, 205–214. [CrossRef]
132. Andreeva, D.; Petrova, P.; Ilieva, L.; Sobczak, J.W.; Abrashev, M.V. Design of new gold catalysts supported on mechanochemically activated ceria-alumina, promoted by molybdena for complete benzene oxidation. *Appl. Catal. B* **2008**, *77*, 364–372. [CrossRef]
133. Andreeva, D.; Petrova, P.; Sobczak, J.W.; Ilieva, L.; Abrashev, M. Gold supported on ceria and ceria–alumina promoted by molybdena for complete benzene oxidation. *Appl. Catal. B* **2006**, *67*, 237–245. [CrossRef]

134. Avgouropoulos, G.; Manzoli, M.; Boccuzzi, F.; Tabakova, T.; Papavasiliou, J.; Ioannides, T.; Idakiev, V. Catalytic performance and characterization of Au/doped-ceria catalysts for the preferential CO oxidation reaction. *J. Catal.* **2008**, *256*, 237–247. [CrossRef]
135. Ghosh, P.; Camellone, M.F.; Fabris, S. Fluxionality of Au clusters at ceria surfaces during CO oxidation: Relationships among reactivity, size, cohesion, and surface defects from DFT simulations. *J. Phys. Chem. Lett.* **2013**, *4*, 2256–2263. [CrossRef]
136. Andreeva, D.; Idakiev, V.; Tabakova, T.; Ilieva, L.; Falaras, P.; Bourlinos, A.; Travlos, A. Low-temperature water-gas shift reaction over Au/CeO_2 catalysts. *Catal. Today* **2002**, *72*, 51–57. [CrossRef]
137. Vindigni, F.; Manzoli, M.; Tabakova, T.; Idakiev, V.; Boccuzzi, F.; Chiorino, A. Gold catalysts for low temperature water-gas shift reaction: Effect of ZrO_2 addition to CeO_2 support. *Appl. Catal. B* **2012**, *125*, 507–515. [CrossRef]
138. Si, R.; Flytzani-Stephanopoulos, M. Shape and crystal-plane effects of nanoscale ceria on the activity of Au-CeO_2 catalysts for the water-gas shift reaction. *Angew. Chem. Int. Ed.* **2008**, *47*, 2884–2887. [CrossRef] [PubMed]
139. Zhao, X.; Ma, S.; Hrbek, J.; Rodriguez, J.A. Reaction of water with Ce–Au(111) and CeO_x/Au(111) surfaces: Photoemission and STM studies. *Surf. Sci.* **2007**, *601*, 2445–2452. [CrossRef]
140. Reina, T.R.; Ivanova, S.; Delgado, J.J.; Ivanov, I.; Idakiev, V.; Tabakova, T.; Centeno, M.A.; Odriozola, J.A. Viability of Au/CeO_2–ZnO/Al_2O_3 catalysts for pure hydrogen production by the water-gas shift reaction. *ChemCatChem* **2014**, *6*, 1401–1409.
141. Reina, T.R.; Castaño, M.G.; Palma, S.; Ivanova, S.; Odriozola, J.A. Twenty years of golden future in the water gas shift reaction. In *Heterogeneous Gold Catalysts and Catalysis*; Ma, Z., Dai, S., Eds.; The Royal Society of Chemistry: London, UK, 2014; pp. 111–139.
142. Reina, T.R.; Ivanova, S.; Centeno, M.A.; Odriozola, J.A. Boosting the activity of a Au/CeO_2/Al_2O_3 catalyst for the WGS reaction. *Catal. Today* **2015**, *253*, 149–154. [CrossRef]
143. Reina, T.R.; Ivanova, S.; Centeno, M.A.; Odriozola, J.A. Catalytic screening of Au/CeO_2-MO_x/Al_2O_3 catalysts (M = La, Ni, Cu, Fe, Cr, Y) in the CO–PrOx reaction. *Int. J. Hydrog. Energy* **2015**, *40*, 1782–1788. [CrossRef]
144. Reina, T.R.; Ivanova, S.; Centeno, M.A.; Odriozola, J.A. The role of Au, Cu & CeO_2 and their interactions for an enhanced WGS performance. *Appl. Catal. B* **2016**, *187*, 98–107.
145. Lu, J.L.; Gao, H.J.; Shaikhutdinov, S.; Freund, H.J. Gold supported on well-ordered ceria films: Nucleation, growth and morphology in CO oxidation reaction. *Catal. Lett.* **2007**, *114*, 8–16. [CrossRef]
146. Rodriguez, J.A. Gold-based catalysts for the water–gas shift reaction: Active sites and reaction mechanism. *Catal. Today* **2011**, *160*, 3–10. [CrossRef]
147. Deng, W.; Jesus, J.D.; Saltsburg, H.; Flytzani-Stephanopoulos, M. Low-content gold–ceria catalysts for the water–gas shift and preferential CO oxidation reactions. *Appl. Catal. A* **2005**, *291*, 126–135. [CrossRef]
148. Casaletto, M.P.; Longo, A.; Martorana, A.; Prestianni, A.; Venezia, A.M. XPS study of supported gold catalysts: The role of Au° and Au^{+d} species as active sites. *Surf. Interface Anal.* **2006**, *38*, 215–218. [CrossRef]
149. Rodriguez, J.A.; Pérez, M.; Evans, J.; Liu, G.; Hrbek, J. Reaction of SO_2 with Au/CeO_2(111): Importance of O vacancies in the activation of gold. *J. Chem. Phys.* **2005**, *122*, 241101. [CrossRef] [PubMed]
150. Domínguez, M.I.; Sanchez, M.; Centeno, M.A.; Montes, M.; Odriozola, J.A. 2-Propanol oxidation over gold supported catalysts coated ceramic foams prepared from stainless steel wastes. *J. Mol. Catal. A* **2007**, *277*, 145–154. [CrossRef]
151. Konya, Z.; Puntes, V.F.; Kiricsi, I.; Zhu, J.; Ager, J.W.; Ko, M.K.; Frei, H.; Alivisatos, P.; Somorjai, G.A. Synthetic insertion of gold nanoparticles into mesoporous silica. *Chem. Mat.* **2003**, *15*, 1242–1248. [CrossRef]
152. Lai, S.-Y.; Qiu, Y.; Wang, S. Effects of the structure of ceria on the activity of gold/ceria catalysts for the oxidation of carbon monoxide and benzene. *J. Catal.* **2006**, *237*, 303–313. [CrossRef]
153. Courtois, X.; Bion, N.; Marécot, P.; Duprez, D. The role of cerium-based oxides used as oxygen storage materials in DeNOx catalysis. In *Studies in Surface Science and Catalysis*; Granger, P., Pârvulescu, V.I., Eds.; Elsevier: Amsterdam, The Netherlands, 2007; pp. 235–259.
154. Yao, H.C.; Yao, Y.F.Y. Ceria in automotive exhaust catalysts: I. Oxygen storage. *J. Catal.* **1984**, *86*, 254–265. [CrossRef]
155. Fonseca, J.D.S.L.; Ferreira, H.S.; Bion, N.; Pirault-Roy, L.; Rangel, M.D.C.; Duprez, D.; Epron, F. Cooperative effect between copper and gold on ceria for CO–PROX reaction. *Catal. Today* **2012**, *180*, 34–41. [CrossRef]

156. Hammer, B.; Norskov, J.K. Why gold is the noblest of all the metals. *Nature* **1995**, *376*, 238–240. [CrossRef]
157. Hutchings, G.J. Vapor phase hydrochlorination of acetylene: Correlation of catalytic activity of supported metal chloride catalysts. *J. Catal.* **1985**, *96*, 292–295. [CrossRef]
158. Schubert, M.M.; Hackenberg, S.; van Veen, A.C.; Muhler, M.; Plzak, V.; Behm, R.J. CO oxidation over supported gold catalysts—"Inert" and "active" support materials and their role for the oxygen supply during reaction. *J. Catal.* **2001**, *197*, 113–122. [CrossRef]
159. Laguna, O.H.; Domínguez, M.I.; Centeno, M.A.; Odriozola, J.A. Forced deactivation and postmortem characterization of a metallic microchannel reactor employed for the preferential oxidation of CO (PROX). *Chem. Eng. J.* **2016**, *302*, 650–662. [CrossRef]
160. Laguna, O.H.; Ngassa, E.M.; Oraá, S.; Álvarez, A.; Domínguez, M.I.; Romero-Sarria, F.; Arzamendi, G.; Gandía, L.M.; Centeno, M.A.; Odriozola, J.A. Preferential oxidation of CO (CO–PROX) over CuO_x/CeO_2 coated microchannel reactor. *Catal. Today* **2012**, *180*, 105–110. [CrossRef]
161. Reina, T.R.; Megías-Sayago, C.; Florez, A.P.; Ivanova, S.; Centeno, M.Á.; Odriozola, J.A. H_2 oxidation as criterion for PrOx catalyst selection: Examples based on Au–CoO_x-supported systems. *J. Catal.* **2015**, *326*, 161–171. [CrossRef]
162. Avgouropoulos, G.; Ioannides, T. TPD and TPSR study of CO interaction with CuO–CeO_2 catalysts. *J. Mol. Catal. A* **2008**, *296*, 47–53. [CrossRef]
163. Tabakova, T.; Manzoli, M.; Paneva, D.; Boccuzzi, F.; Idakiev, V.; Mitov, I. CO-free hydrogen production over Au/CeO_2–Fe_2O_3 catalysts: Part 2. Impact of the support composition on the performance in the water-gas shift reaction. *Appl. Catal. B* **2011**, *101*, 266–274. [CrossRef]
164. Xiao, G.; Li, S.; Li, H.; Chen, L. Synthesis of doped ceria with mesoporous flowerlike morphology and its catalytic performance for CO oxidation. *Microporous Mesoporous Mater.* **2009**, *120*, 426–431. [CrossRef]
165. Rodriguez, J.A.; Ma, S.; Liu, P.; Hrbek, J.; Evans, J.; Perez, M. Activity of CeO_x and TiO_x nanoparticles grown on Au(111) in the water-gas shift reaction. *Science* **2007**, *318*, 1757–1760. [CrossRef] [PubMed]
166. Wang, Y.; Hwang, G.S. Adsorption of Au atoms on stoichiometric and reduced TiO_2(110) rutile surfaces: A first principles study. *Surf. Sci.* **2003**, *542*, 72–80. [CrossRef]
167. Zhang, C.; Michaelides, A.; King, D.A.; Jenkins, S.J. Anchoring sites for initial Au nucleation on CeO_2{111}: O vacancy versus Ce vacancy. *J. Phys. Chem. C* **2009**, *113*, 6411–6417. [CrossRef]
168. Tabakova, T.; Boccuzzi, F.; Manzoli, M.; Andreeva, D. FTIR study of low-temperature water-gas shift reaction on gold/ceria catalyst. *Appl. Catal. A* **2003**, *252*, 385–397. [CrossRef]
169. Wahlström, E.; Lopez, N.; Schaub, R.; Thostrup, P.; Ronnau, A.; Africh, C.; Laegsgaard, E.; Norskov, J.K.; Besenbacher, F. Bonding of gold nanoclusters to oxygen vacancies on rutile TiO_2(110). *Phys. Rev. Lett.* **2003**. [CrossRef] [PubMed]
170. Guzman, J.; Carrettin, S.; Fierro-Gonzalez, J.C.; Hao, Y.L.; Gates, B.C.; Corma, A. CO oxidation catalyzed by supported gold: Cooperation between gold and nanocrystalline rare-earth supports forms reactive surface superoxide and peroxide species. *Angew. Chem. Int. Ed.* **2005**, *44*, 4778–4781. [CrossRef] [PubMed]
171. Long, R.Q.; Huang, Y.P.; Wan, H.L. Surface oxygen species over cerium oxide and their reactivities with methane and ethane by means of in situ confocal microprobe Raman spectroscopy. *J. Raman Spectrosc.* **1997**, *28*, 29–32. [CrossRef]
172. Penkova, A.; Laguna, O.H.; Centeno, M.A.; Odriozola, J.A. CO-induced morphology changes in Zn-modified ceria: A FTIR spectroscopic study. *J. Phys. Chem. C* **2012**, *116*, 5747–5756. [CrossRef]
173. Wuilloud, E.; Delley, B.; Schneider, W.D.; Baer, Y. Spectroscopic evidence for localized and extended F-symmetry states in CeO_2. *Phys. Rev. Lett.* **1984**, *53*, 202–205. [CrossRef]
174. Panhans, M.A.; Blumenthal, R.N. A thermodynamic and electrical conductivity study of nonstoichiometric cerium dioxide. *Solid State Ion.* **1993**, *60*, 279–298. [CrossRef]
175. Binet, C.; Badri, A.; Lavalley, J.C. A spectroscopic characterization of the reduction of ceria from electronic-transitions of intrinsic point-defects. *J. Phys. Chem.* **1994**, *98*, 6392–6398. [CrossRef]
176. Gamarra, D.; Martínez-Arias, A. Preferential oxidation of CO in rich H_2 over CuO/CeO_2: Operando-DRIFTS analysis of deactivating effect of CO_2 and H_2O. *J. Catal.* **2009**, *263*, 189–195. [CrossRef]
177. Reina, T.R.; Ivanova, S.; Idakiev, V.; Delgado, J.J.; Ivanov, I.; Tabakova, T.; Centeno, M.A.; Odriozola, J.A. Impact of Ce–Fe synergism on the catalytic behaviour of Au/CeO_2–FeO_x/Al_2O_3 for pure H_2 production. *Catal. Sci. Technol.* **2013**, *3*, 779–787.

178. Sudarsanam, P.; Mallesham, B.; Reddy, P.S.; Großmann, D.; Grünert, W.; Reddy, B.M. Nano-Au/CeO_2 catalysts for CO oxidation: Influence of dopants (Fe, La and Zr) on the physicochemical properties and catalytic activity. *Appl. Catal. B* **2014**, *144*, 900–908. [CrossRef]
179. Gamarra, D.; Hornés, A.; Koppány, Z.; Schay, Z.; Munuera, G.; Soria, J.; Martínez-Arias, A. Catalytic processes during preferential oxidation of CO in H_2-rich streams over catalysts based on copper–ceria. *J. Power Sources* **2007**, *169*, 110–116. [CrossRef]
180. Hao, Y.; Yang, C.K.; Haile, S.M. Ceria-zirconia solid solutions ($Ce_{1-x}Zr_xO_2$-delta, $x \leq 0.2$) for solar thermochemical water splitting: A thermodynamic study. *Chem. Mat.* **2014**, *26*, 6073–6082. [CrossRef]
181. Wang, Q.; Zhao, B.; Li, G.; Zhou, R. Application of rare earth modified Zr-based ceria-zirconia solid solution in three-way catalyst for automotive emission control. *Environ. Sci. Technol.* **2010**, *44*, 3870–3875. [CrossRef] [PubMed]
182. Wang, Q.; Li, G.; Zhao, B.; Zhou, R. The effect of rare earth modification on ceria–zirconia solid solution and its application in Pd-only three-way catalyst. *J. Mol. Catal. A* **2011**, *339*, 52–60. [CrossRef]
183. Liang, S.; Veser, G. Mixed lanthana/ceria nanorod-supported gold catalysts for water-gas-shift. *Catal. Lett.* **2012**, *142*, 936–945. [CrossRef]
184. Fu, Q.; Deng, W.; Saltsburg, H.; Flytzani-Stephanopoulos, M. Activity and stability of low-content gold–cerium oxide catalysts for the water–gas shift reaction. *Appl. Catal. B* **2005**, *56*, 57–68. [CrossRef]
185. Hilaire, S.; Wang, X.; Luo, T.; Gorte, R.J.; Wagner, J. A comparative study of water-gas-shift reaction over ceria supported metallic catalysts. *Appl. Catal. A* **2001**, *215*, 271–278. [CrossRef]
186. Hori, C.E.; Permana, H.; Ng, K.Y.S.; Brenner, A.; More, K.; Rahmoeller, K.M.; Belton, D. Thermal stability of oxygen storage properties in a mixed CeO_2–ZrO_2 system. *Appl. Catal. B* **1998**, *16*, 105–117. [CrossRef]
187. Dutta, G.; Waghmare, U.V.; Baidya, T.; Hegde, M.S.; Priolkar, K.R.; Sarode, P.R. Reducibility of $Ce_{1-x}Zr_xO_2$: Origin of enhanced oxygen storage capacity. *Catal. Lett.* **2006**, *108*, 165–172. [CrossRef]
188. Gamboa-Rosales, N.K.; Ayastuy, J.L.; González-Marcos, M.P.; Gutiérrez-Ortiz, M.A. Oxygen-enhanced water gas shift over ceria-supported Au–Cu bimetallic catalysts prepared by wet impregnation and deposition–precipitation. *Int. J. Hydrog. Energy* **2012**, *37*, 7005–7016. [CrossRef]
189. Gamboa-Rosales, N.K.; Ayastuy, J.L.; Iglesias-González, A.; González-Marcos, M.P.; Gutiérrez-Ortiz, M.A. Oxygen-enhanced WGS over ceria-supported Au–Co_3O_4 bimetallic catalysts. *Chem. Eng. J.* **2012**, *207–208*, 49–56. [CrossRef]
190. Hurtado-Juan, M.-A.; Yeung, C.M.Y.; Tsang, S.C. A study of co-precipitated bimetallic gold catalysts for water–gas shift reaction. *Catal. Commun.* **2008**, *9*, 1551–1557. [CrossRef]
191. Deng, W.L.; Flytzani-Stephanopoulos, M. On the issue of the deactivation of Au/ceria and Pt-ceria water-gas shift catalysts in practical fuel-cell applications. *Angew. Chem. Int. Ed.* **2006**, *45*, 2285–2289. [CrossRef] [PubMed]
192. González-Castaño, M.; Reina, T.R.; Ivanova, S.; Tejada, L.M.M.; Centeno, M.A.; Odriozola, J.A. O_2-assisted water gas shift reaction over structured Au and Pt catalysts. *Appl. Catal. B* **2016**, *185*, 337–343. [CrossRef]
193. Arbeláez, O.; Reina, T.R.; Ivanova, S.; Bustamante, F.; Villa, A.L.; Centeno, M.A.; Odriozola, J.A. Mono and bimetallic Cu–Ni structured catalysts for the water gas shift reaction. *Appl. Catal. A* **2015**, *497*, 1–9. [CrossRef]
194. Giroux, T.; Hwang, S.; Liu, Y.; Ruettinger, W.; Shore, L. Monolithic structures as alternatives to particulate catalysts for the reforming of hydrocarbons for hydrogen generation. *Appl. Catal. B* **2005**, *56*, 95–110. [CrossRef]
195. Colussi, S.; Katta, L.; Amoroso, F.; Farrauto, R.J.; Trovarelli, A. Ceria-based palladium zinc catalysts as promising materials for water gas shift reaction. *Catal. Commun.* **2014**, *47*, 63–66. [CrossRef]
196. Luengnaruemitchai, A.; Osuwan, S.; Gulari, E. Selective catalytic oxidation of CO in the presence of H_2 over gold catalyst. *Int. J. Hydrog. Energy* **2004**, *29*, 429–435. [CrossRef]
197. Kahlich, M.J.; Gasteiger, H.A.; Behm, R.J. Kinetics of the selective low-temperature oxidation of CO in H_2-rich gas over Au/α-Fe_2O_3. *J. Catal.* **1999**, *182*, 430–440. [CrossRef]
198. Lin, S.D.; Bollinger, M.; Vannice, M.A. Low-temperature CO oxidation over Au/TiO_2 and Au/SiO_2 catalysts. *Catal. Lett.* **1993**, *17*, 245–262. [CrossRef]
199. Liao, X.; Chu, W.; Dai, X.; Pitchon, V. Bimetallic Au–Cu supported on ceria for PROX reaction: Effects of Cu/Au atomic ratios and thermal pretreatments. *Appl. Catal. B* **2013**, *142–143*, 25–37. [CrossRef]
200. Carriazo, J.G.; Martínez, L.M.; Odriozola, J.A.; Moreno, S.; Molina, R.; Centeno, M.A. Gold supported on Fe, Ce, and Al pillared bentonites for CO oxidation reaction. *Appl. Catal. B* **2007**, *72*, 157–165. [CrossRef]

201. Costello, C.K.; Yang, J.H.; Law, H.Y.; Wang, Y.; Lin, J.N.; Marks, L.D.; Kung, M.C.; Kung, H.H. On the potential role of hydroxyl groups in CO oxidation over Au/Al_2O_3. *Appl. Catal. A* **2003**, *243*, 15–24. [CrossRef]
202. Fujitani, T.; Nakamura, I.; Haruta, M. Role of water in CO oxidation on gold catalysts. *Catal. Lett.* **2014**, *144*, 1475–1486. [CrossRef]
203. Avgouropoulos, G.; Ioannides, T.; Papadopoulou, C.; Batista, J.; Hocevar, S.; Matralis, H.K. A comparative study of Pt/gamma-Al_2O_3, Au/alpha-Fe_2O_3 and CuO–CeO_2 catalysts for the selective oxidation of carbon monoxide in excess hydrogen. *Catal. Today* **2002**, *75*, 157–167. [CrossRef]